NTNU

Norwegian University of
Science and Technology

Determination of nitrated and oxygenated polycyclic aromatic hydrocarbons in arctic air by GC/NICI-MS

Kristin Sundby

Chemical Engineering and Biotechnology
Submission date: June 2017
Supervisor: Rudolf Schmid, IKJ
Co-supervisor: Roland Kallenborn, UNIS/NMBU

Norwegian University of Science and Technology
Department of Chemistry

Preface

This master thesis in analytical chemistry was written at the Department of Chemistry at the Norwegian University of Science and Technology (NTNU) in collaboration with the Department of Arctic Technology at the University Centre in Svalbard (UNIS). The analyses were carried out at the Faculty of Chemistry, Biotechnology and Food Science at the Norwegian University of Life Sciences (NMBU). The project was collocated with the PhD project of MSc. Tatiana Drotikova at UNIS.

Trondheim, June 2017

Kristin Sundby

UNIS - The University Centre in Svalbard

NTNU
Norwegian University of
Science and Technology

Norwegian University
of Life Sciences

Acknowledgements

This semester has been a journey and I feel fortunate for all the people I have met and all the places I have visited during my master project.

First, I would like to thank my supervisor Prof. Roland Kallenborn for giving me the opportunity to work with this project. Thank you for your guidance during my stay in Svalbard and during the analytical work at NMBU. Also, thank you to my supervisor at NTNU, Assoc. Prof. Rudolf Schmid, for helping me with the organization of the master project, in addition to giving me valuable feedback in the writing process.

I am truly grateful for all the people at UNIS who helped me during my stay in Svalbard; I could never have done this work without you. Thanks to PhD candidate Tatiana Drotikova for everything you have arranged for me and all advice during my work. Thanks to the Technical and Logistics Department for logistical assistance in my field and laboratory work. Thanks to all of you who joined me in the field, carrying the ladder and looking out for polar bears. A special thanks to Dr. Anne Karine Halse who has been an incredible support. I would also like to thank Assoc. Prof. Mark Hermanson for the air sampling equipment. Moreover, thanks to Nina Mosesen Hansen in the reception for always having a car ready for me when I had to go out in the field!

I was lucky to be welcomed at the Faculty of Chemistry, Biotechnology and Food Science at NMBU. Thanks to all of you for introducing me to your facilities and including me in your lunch hours.

Last, but not least, thank you to all of my fellow students at NTNU for five marvelous years together. Thanks to my friends at Demokrit for encouragements during the long days finishing our theses. You are a fantastic group of people and bake the most delicious cakes.

Abstract

Nitrated and oxygenated polycyclic aromatic hydrocarbons (nitro- and oxy-PAHs) are pollutants that enter the atmosphere from incomplete combustions and from degradation of regular PAHs. Nowadays, there are growing interests of atmospheric concentrations of nitro- and oxy-PAHs because of their high potential mutagenicity and carcinogenicity. In this study, a method has been tested for determination of 21 nitro-PAHs and 11 oxy-PAHs in particulate and gaseous phase of air samples from Longyearbyen, Svalbard, Norway. The samples were collected by high volume air sampling during February and March 2017. The sample work up procedure involved a Quick Easy Cheap Effective Rugged and Safe (QuEChERS) approach for extraction of particulate phase compounds, while the compounds in gaseous phase were extracted by the more traditional Soxhlet extraction. Analyses were carried out by gas chromatography/mass spectrometry with negative ion chemical ionization (GC/NICI-MS).

The analytical method was suitable for detection and quantification of nitro- and oxy-PAHs of low molecular weight. However, further method optimization is necessary in order to identify and quantify compounds of higher molecular weight, as the sensitivity decreased with increasing retention time. The total concentration of nitro- and oxy-PAHs in ambient air of Longyearbyen varied from 68.3 to 611.4 pg m^{-3}, which is far below concentrations reported in literature from other sites. Analytes were mainly detected in particulate phase, except 1- and 2-nitronaphthalene. 9-Fluorenone was the most abundant compound, which correlates with research from other sites. In aspect of different weather conditions, the findings of this study indicates that both emissions from the coal power plant and emissions from traffic are important sources of atmospheric nitro- and oxy-PAHs in Longyearbyen.

Sammendrag

Nitrerte og oksygenerte polysykliske aromatiske hydrokarboner (nitro- og oksy-PAH'er) er forurensende forbindelser som slippes ut i atmosfæren gjennom ufullstendige forbrenningsprosesser. De kan også dannes i atmosfæren ved nedbryting av polysykliske aromatiske hydrokarboner. Konsentrasjonen av nitro- og oksy-PAH'er i luft er av økende interesse i miljøanalyser, da disse forbindelsene kan ha mutagene og kreftfremkallende egenskaper. I denne oppgaven har en metode blitt testet for bestemmelse av 21 nitro-PAH'er og 11-oksy-PAH'er i partikkel- og gassfase i luftprøver fra Longyearbyen, Svalbard, Norge. Luftprøver ble tatt ved aktiv prøvetaking i februar og mars 2017. Prøveopparbeidelsen besto av en metode kalt "QuEChERS" (Quick Easy Cheap Effective Rugged and Safe) for ekstraksjon av forbindelser i partikkelfase, mens forbindelser i gassfase ble ekstrahert ved tradisjonell Soxhlet ekstraksjon. Analysene ble utført med gass kromatografi/massespektrometri med negativ kjemisk ionisering (GC/NICI-MS).

Den analytiske metoden var egnet for identifisering og kvantifisering av nitro- og oksy-PAH'er med lav molekylvekt. Derimot er videre metodeoptimering nødvendig for å kunne identifisere og kvantifisere forbindelser med høyere molekylvekt, da sensitiviteten avtok med økende retensjonstid. Total konsentrasjon av nitro- og oksy-PAH'er i luften i Longyearbyen varierte fra 68,3 til 611,4 pg m^{-3}, som er mye lavere enn litteraturdata fra andre områder i verden. De fleste forbindelser ble funnet i partikkelfase, bortsett fra 1- og 2-nitronaftalen. 9-Fluorenon utgjorde den største andelen av den totale konsentrasjonen av nitro- og oksy-PAH'er, noe som stemmer overens med tidligere forskning i andre områder. I lys av ulike værforhold indikerer resultatene fra denne oppgaven at både utslipp fra kullkraftverket og trafikk er viktige kilder til nitro- og oksy-PAH'er i lufta i Longyearbyen.

Table of contents

List of figures

List of tables

Acronyms and abbreviations

AC	Alternating current
ACN	Acetonitrile
APCI	Atmospheric pressure chemical ionization
CAS	Chemical abstracts service
CI	Chemical ionization
DC	Direct current
DCM	Dichloromethane
ECD	Electron capture detector
EI	Electron ionization
GPS	Global positioning system
GC	Gas chromatography
GLC	Gas-liquid chromatography
GSC	Gas-solid chromatography
h	hour
HPLC	High performance liquid chromatography
ISTD	Internal standard
IUPAC	International Union of Pure and Applied Chemistry
LOD	Limit of detection
LOQ	Limit of quantification
m	meter
mL	milliliter
MS	Mass spectrometry
ms	milliseconds
MW	Molecular weight
n.d.	not detected *or* no date
n.q.	not quantified
ng	nanogram
NICI	Negative ion chemical ionization
NMBU	Norwegian University of Life Sciences
NTNU	Norwegian University of Science and Technology
PAH	Polycyclic aromatic hydrocarbon

pg	picogram
PLE	Pressurized liquid extraction
PUF	Polyurethane foam
QFF	Quartz fiber filter
QRR	Qualifier response ratio
QuEChERS	Quick Easy Cheap Effective Rugged and Safe
RSTD	Recovery standard
rpm	revolutions per minute
S/N	Signal-to-noise ratio
SFE	Supercritical fluid extraction
SIM	Selected ion monitoring
SPE	Solid-phase extraction
SVOC	Semi-volatile organic compound
TIC	Total ion chromatogram
µL	microliter
µm	micrometer
UNIS	University Centre in Svalbard
WCOT	Wall-coated open tubular

1 Introduction

1.1 Background

Polycyclic aromatic hydrocarbons (PAHs) are organic compounds that have been an environmental concern for several decades, as they were one of the first groups of pollutants to be identified as toxic chemicals (Keith and Telliard, 1979). Today, it is well known that many PAHs have carcinogenic and mutagenic properties, which have led to regulations of emissions and allowable concentrations of PAHs in air (Kim et al., 2013). However, more recent research reports that derivatives of PAHs, such as nitrated PAHs (nitro-PAHs) and oxygenated PAHs (oxy-PAHs), can be even more toxic than their parent PAHs (Durant et al., 1996; Arey, 1998). Consequently, there are growing interests on the levels and sources of nitro- and oxy-PAHs in the environment.

Nitro- and oxy-PAHs enter the atmosphere from direct emissions, such as coal and biomass combustions, or from degradation reactions of PAHs (Zhuo et al., 2017). This study took place in Longyearbyen, a small Arctic settlement that obtains its electric power and district heating from its own coal power plant, located in town (Longyearbyen Lokalstyre, 2012). The power plant is therefore expected to be the main emission source for PAHs and their derivatives in Longyearbyen, but these pollutants may also be emitted from vehicles, airplanes and boats. So far, levels of nitro- and oxy-PAHs have not been documented in this area.

The atmospheric concentrations of nitro- and oxy-PAHs in rural areas are usually of trace levels. A reliable method for sampling, sample preparation and analysis is important in order to assess their presence. Nitro- and oxy-PAHs are mainly sampled by high volume air samplers, where particulate phase PAHs are collected on filters, while gas phase PAHs are collected in solid sorbents. Furthermore, the analytes are extracted from the matrix into a solvent, followed by a clean-up procedure and volume reduction. Methods used for the separation and detection of nitro- and oxy-PAHs include liquid or gas chromatography coupled with a variety of detectors (Kielhorn et al., 2004).

1.2 Objectives

The main objectives of this master's thesis were:

1. Validation of an analytical method for the quantitative determination of nitro- and oxy-PAHs in air samples by GC/NICI-MS (gas chromatography/mass spectrometry with negative ion chemical ionization)
2. Implementation of a newly developed QuEChERS (Quick Easy Cheap Effective Rugged and Safe) approach for extraction of organic aerosols
3. Application of the validated method for the quantification of nitro- and oxy-PAHs in ambient air from Longyearbyen, Svalbard, Norway

2 Theory

2.1 Nitro- and oxy-PAHs

2.1.1 Identity, physical and chemical properties

Nitrated polycyclic aromatic hydrocarbons (nitro-PAHs) and oxygenated polycyclic aromatic hydrocarbons (oxy-PAHs) are derivatives of PAHs. PAHs are compounds containing two or more fused aromatic rings of carbon and hydrogen atoms. Nitro-PAHs and oxy-PAHs occur in the atmosphere as a mixture together with parent PAHs (Kielhorn et al., 2004). These compounds are semi-volatile organic compounds (SVOCs), which are defined as organic molecules that can have meaningful abundances in both gas and condensed phases (Weschler and Nazaroff, 2008). Consequently, they appear either in vapor phase or adsorbed to particulate matter in the atmosphere, depending on their vapor pressure and the ambient conditions (such as temperature, humidity and presence of aerosols) (Kielhorn et al., 2004; Lundstedt et al., 2007; Kim et al., 2013). Nitro-PAHs are usually present in smaller quantities (by two orders of magnitude) than PAHs (Durant et al., 1996; Niederer, 1998; Kielhorn et al., 2004; Zhang et al., 2011), while oxy-PAHs have been reported at concentrations close to levels found for parent PAHs (Durant et al., 1996; Niederer, 1998; Lundstedt et al., 2007).

Nitro-PAHs consist of two or more fused aromatic rings substituted with at least one nitro group ($-NO_2$) (Kielhorn et al., 2004). The structural formulas of the selected nitro-PAHs in this study are shown in Figure 2.1. The carcinogen 9-methylcarbazole and the mutagen 4-nitrobiphenyl were also included in the study and are presented among the nitro-PAHs, although they are not defined as nitro-PAHs considering their structural formulas. However, they have similar properties as nitro-PAHs and are possible toxic air pollutants (Watson et al., 1988, p.562; Pohanish, 2008, p.1960).

Oxy-PAHs are defined as PAHs with one or more carbonyl groups (=O) attached to the aromatic ring structure. They can also contain other functional groups, such as 2-methyl-9,10-anthraquinone that is substituted with an alkyl group ($-CH_3$) (Lundstedt et al., 2007). The structural formulas of the selected oxy-PAHs are shown in Figure 2.2. Table 2.1 presents the nomenclature, molecular formula and relative molecular mass of each target nitro- and oxy-PAH in this study.

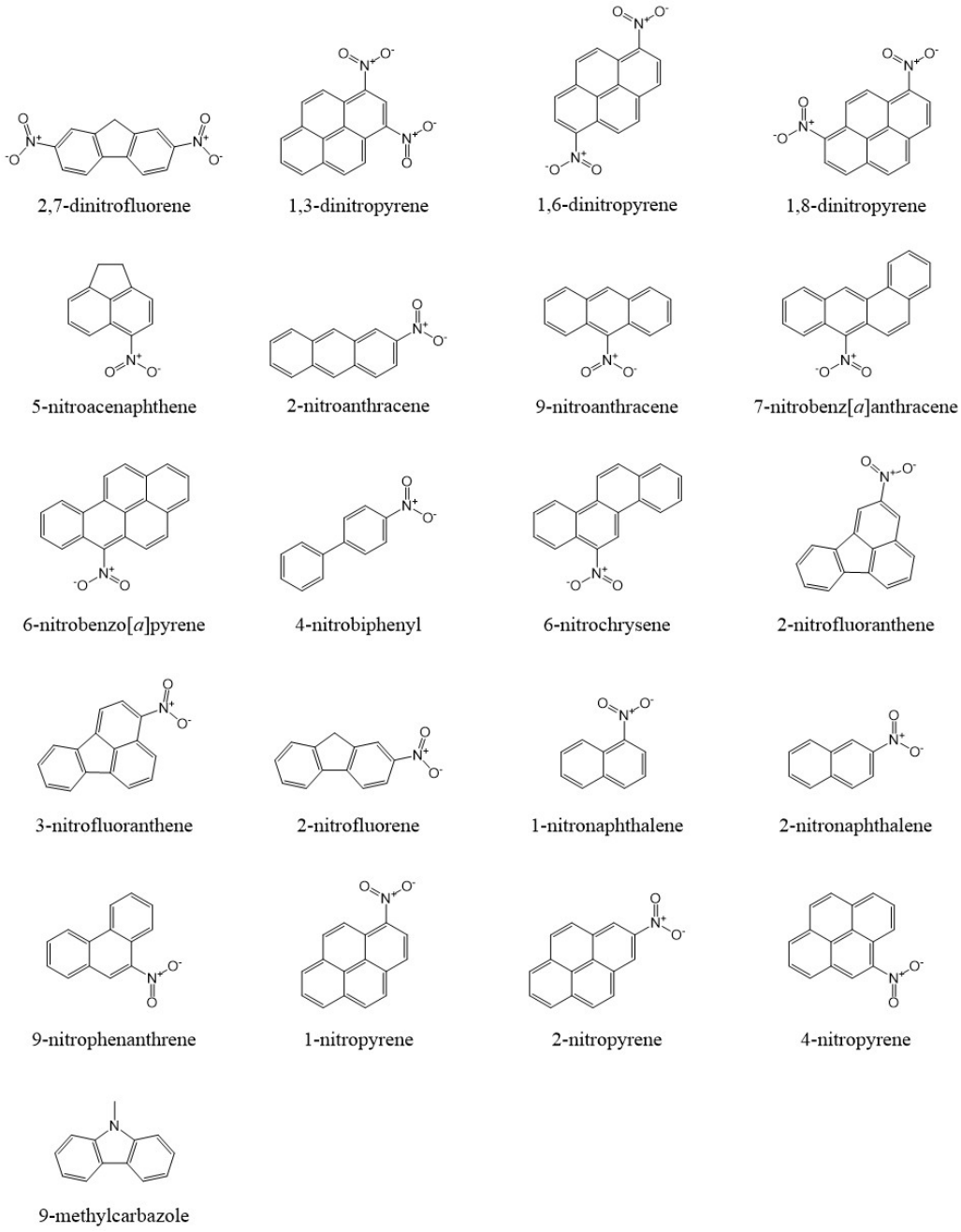

Figure 2.1: Molecular structures of the target nitro-PAHs in this study.

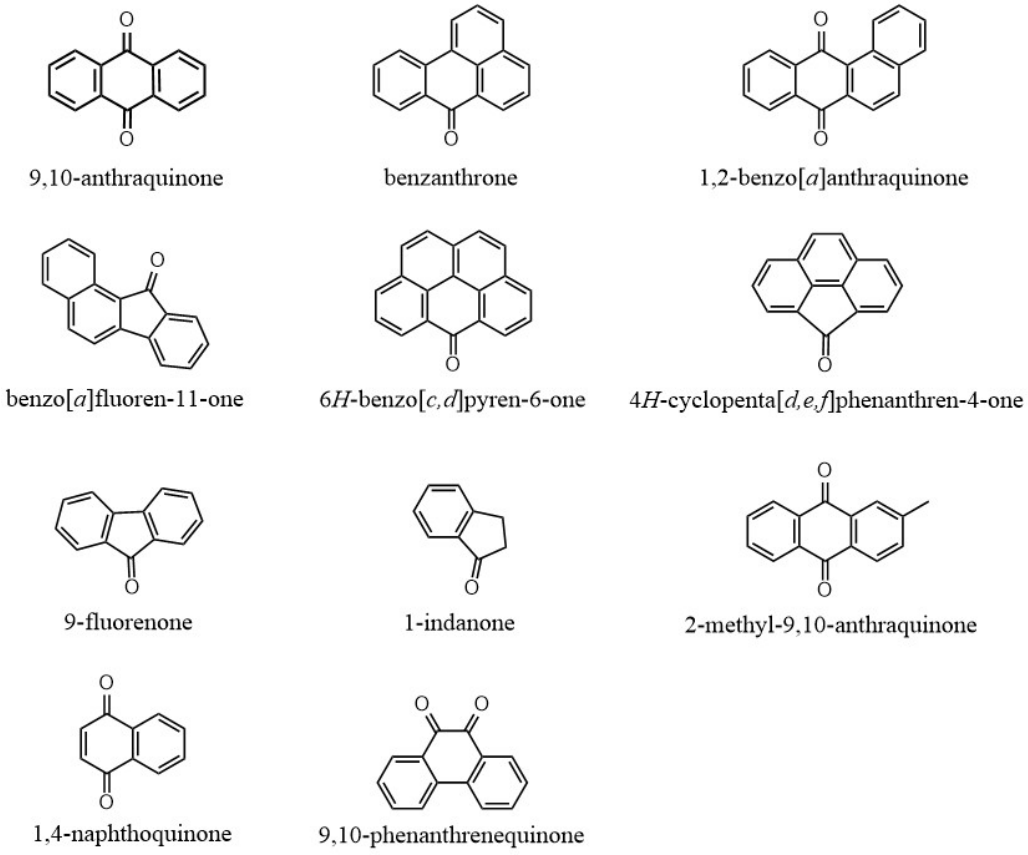

Figure 2.2: Molecular structures of the target oxy-PAHs in this study.

Table 2.1: Nomenclature, molecular formula and relative molecular mass of each target compound.

Parent PAH	Name	Molecular Formula	MW[a]
Nitro-PAHs			
Two-ring PAHs			
Biphenyl	4-Nitrobiphenyl	$C_{12}H_9NO_2$	199.21
Naphthalene	1-Nitronaphthalene	$C_{10}H_7NO_2$	173.17
	2-Nitronaphthalene	$C_{10}H_7NO_2$	173.17
Three-ring PAHs			
Acenaphthene	5-Nitroacenaphthene	$C_{12}H_9NO_2$	199.21
Anthracene	2-Nitroanthracene	$C_{14}H_9NO_2$	223.23
	9-Nitroanthracene	$C_{14}H_9NO_2$	223.23
Fluorene	2-Nitrofluorene	$C_{13}H_9NO_2$	211.22
	2,7-Dinitrofluorene	$C_{13}H_8N_2O_4$	256.21
Phenanthrene	9-Nitrophenanthrene	$C_{14}H_9NO_2$	223.23
-	9-Methylcarbazole	$C_{13}H_{11}N$	181.23
Four-ring PAHs			
Fluoranthene	2-Nitrofluoranthene	$C_{16}H_9NO_2$	247.25
	3-Nitrofluoranthene	$C_{16}H_9NO_2$	247.25
Pyrene	1-Nitropyrene	$C_{16}H_9NO_2$	247.25
	2-Nitropyrene	$C_{16}H_9NO_2$	247.25
	4-Nitropyrene	$C_{16}H_9NO_2$	247.25
	1,3-Dinitropyrene	$C_{16}H_8N_2O_4$	292.25
	1,6-Dinitropyrene	$C_{16}H_8N_2O_4$	292.25
	1,8-Dinitropyrene	$C_{16}H_8N_2O_4$	292.25
Benz[*a*]anthracene	7-Nitrobenz[*a*]anthracene	$C_{18}H_{11}NO_2$	273.29
Chrysene	6-Nitrochrysene	$C_{18}H_{11}NO_2$	273.29
Five-ring PAHs			
Benzo[*a*]pyrene	6-Nitrobenzo[*a*]pyrene	$C_{20}H_{11}NO_2$	297.31
Oxy-PAHs			
Two-ring PAHs			
Indane	1-Indanone	C_9H_8O	132.16
Naphthalene	1,4-Naphthoquinone	$C_{10}H_6O_2$	158.15
Three-ring PAHs			
Anthracene	9,10-Anthraquinone	$C_{14}H_8O_2$	208.21
	2-Methyl-9,10-anthraquinone	$C_{15}H_{10}O_2$	222.24
Fluorene	9-Fluorenone	$C_{13}H_8O$	180.20
Phenanthrene	9,10-Phenanthrenequinone	$C_{14}H_8O_2$	208.21
Four-ring PAHs			
Benz[*a*]anthracene	1,2-Benz[*a*]anthraquinone	$C_{18}H_{10}O_2$	258.28
Benz[*d,e*]anthracene	Benzanthrone	$C_{17}H_{10}O$	230.27
Benzo[*c*]fluorene	Benzo[*a*]fluoren-11-one	$C_{17}H_{10}O$	230.26
Cyclopenta[*d,e,f*]-phenanthrene	4H-Cyclopenta[*d,e,f*]phenanthren-4-one	$C_{15}H_8O$	204.22
Five-ring PAHs			
Benzo[*c,d*]pyrene	6H-Benzo[*c,d*]pyren-6-one	$C_{19}H_{10}O$	254.28

[a] MW = molecular weight

2.1.2 Sources

PAHs and their derivatives are released into the environment from all forms of incomplete combustions of organic material. Natural sources of PAHs are primarily forest fires and volcanic eruptions. Anthropogenic sources are diverse and include coal and biomass combustion, vehicle emissions and burning of garbage (Zielinska et al., 2004; Kim et al., 2013; Zhuo et al., 2017).

Nitro- and oxy-PAHs can be released from direct emissions (primary sources), as well as derive from chemical degradation reactions of PAHs (secondary sources). A few nitro-PAHs are produced industrially, for example nitronaphthalenes and 5-nitroacenaphthene, which are used primarily as chemical intermediates (Kielhorn et al., 2004).

Particulate nitro-PAHs from combustion processes are formed from high temperature electrophilic nitration of PAHs by nitrogen dioxide (Nielsen, 1984). Nitro-PAHs in vapor phase can be produced by chemical reactions in the presence of nitrogen oxides, initiated by hydroxyl radicals during the day and nitrate radicals at night. Thereupon they might deposit on particulate matter (Arey, 1986; Atkinson et al., 1990). Research reports that atmospheric reactions of PAHs may be the dominant pathway for their degradation in the atmosphere and further become a significant source of nitro-PAHs (Greenberg et al., 1993; Sasaki et al., 1995; Zhang et al., 2011).

Oxy-PAHs are also emitted from incomplete combustion processes, as well as formed through postemission oxidation of PAHs in the atmosphere. This may occur through chemical oxidation and photooxidation with singlet oxygens, hydroxyl radicals, peroxyl radicals or peroxides (Lundstedt et al., 2007). PAHs may also absorb light and undergo direct photooxidation through reactions with ground state oxygen (Mallakin et al., 2000). In addition, oxy-PAHs can be formed through heterogeneous reactions of particulate associated PAHs with ozone (Zhang et al., 2011; Di Filippo et al., 2015).

2.1.3 Fate and transformations in the environment

In general, the distribution of nitro- and oxy-PAHs between particulate phase and gaseous phase is strongly dependent on the molecular weight of the compound (Albinet et al., 2007).

Nitro- and oxy-PAHs may be removed from the atmosphere by deposition to the terrestrial biosphere or by atmospheric degradation (Feilberg and Nielsen, 2000; Kim et al., 2013).

Oxy-PAHs are found to be more persistent in the environment compared to other transformation products of PAHs, and could potentially accumulate as PAHs are degraded. Significant levels of oxy-PAHs have been found in a variety of different matrices in the environment, such as aerosols, sediments, river and coastal waters, industrial waste and soil, which indicates their high persistency in the environment. Due to the fact that oxy-PAHs are more polar than regular PAHs, oxy-PAHs have the ability to spread from contaminated sites via surface water and groundwater (Lundstedt et al., 2007).

Nitro-PAHs are less polar than oxy-PAHs, thus not believed to be transported in water as they have low aqueous solubility. It is rather suggested that particulate nitro-PAHs deposit and adsorb onto soil and sediments, which is similar to the fate of parent PAHs (Kielhorn et al., 2004). The dominant loss process for nitro-PAHs in the atmosphere is photolysis. At night, the main loss process may be particle oxidation by ozone (Feilberg and Nielsen, 2000; Kielhorn et al., 2004).

2.1.4 Toxicity

Many PAHs are well known as carcinogens, mutagens and teratogens and pose a serious threat to human health and wildlife (Boström et al., 2002). Some of the PAH derivatives are regarded as even more toxic than their precursor PAHs, although more research in this field is needed to understand the mechanisms underlying the toxicity (Durant et al., 1996; Lundstedt et al., 2007; Kim et al., 2013).

Several nitro- and oxy-PAHs are shown to be mutagenic, and some of them are potential human carcinogens. A study done by Hayakawa et al. (1997) revealed that up to 50% of total mutagenic activity of diesel particulate extracts is due to the presence of nitro-PAHs. The direct mutagenic activity of tobacco smoke has been highly correlated with the presence of nitro- and oxy-PAHs (Yu et al., 2002). Furthermore, research on the direct mutagenic activity of atmospheric aerosol extracts has also been mainly correlated with nitro- and oxy-PAHs (Bayona et al., 1994; Casellas et al., 1995). The International Agency for Research on Cancer has in-

cluded several nitro-PAHs on the list of possible carcinogens (group 2B) (IARC, 1989).

2.1.5 Air sampling and analytical methods

Environmental analyses of nitro- and oxy-PAHs cannot be carried out without appropriate sample preparation, as the sampling matrices are complex and contain related pollutants that might interfere in instrumental analyses (Kielhorn et al., 2004). The compounds of interest have to be extracted from the sample matrix by a suitable technique. In addition, nitro- and oxy-PAHs are expected to be present at trace levels in the atmosphere, consequently their analyses require several sample preparation steps such as clean-up and pre-concentration (Castells et al., 2003; Albinet et al., 2006; Cochran et al., 2012). The environmental investigations of nitro- and oxy-PAHs are of growing interest, and recent research reports sensitive methods for their identification and quantification in air samples. Some methods are presented below.

Niederer (1998) obtained air samples by high volume sampling using glass fiber filters as sampling medium at a sampling rate of 40 m^3 h^{-1} for 24 hours. The filters were extracted by microwave extraction with methanol:acetone (1:1, v/v), then purified by a combination of reversed and normal solid phase extraction (SPE) with C18 and SiOH as sorbents, respectively. Further clean-up was done by semi-preparative high performance liquid chromatography (HPLC). The analyses of nitro- and oxy-PAHs were carried out by gas chromatography/mass spectrometry (GC/MS) using both electron ionization (EI) and negative ion chemical ionization (NICI).

Castells et al. (2003) collected air particles on glass fiber filters by high volume air sampling at a flow rate of 60 m^3 h^{-1} for 24 hours. A two-step supercritical fluid extraction (SFE) method with CO_2 was developed for simultaneous extraction and purification of nitro- and oxy-PAHs. The results were in agreement with the more conventional method using ultrasonic extraction and SPE clean-up. The analyses were carried out by GC coupled with electron capture detector (ECD) and by GC/MS.

Delhomme et al. (2008) sampled fine particulate matter on quartz fiber filters using a high volume air sampler at a flow rate of 68 m^3 h^{-1} for 24 to 48 hours. Samples were extracted by

ultrasonic agitation without further purification. The analyses were carried out by HPLC using atmospheric pressure chemical ionization (APCI). Tandem MS was shown to give better sensitivity than fluorescence detection.

Cochran et al. (2012) developed a method for trace analysis of parent PAHs and their oxidation products in air particulate matter (diesel exhaust and wood smoke particulate matter). Extractions were performed by Soxhlet extraction sequentially with dichloromethane (DCM) and methanol, and extracts were fractionated and purified by SPE using aminopropyl as sorbent. Determination of nitro- and oxy-PAHs was performed using GC/MS with both EI and NICI ion sources.

Albinet et al. (2014) developed an extraction procedure of particle-bound nitro- and oxy-PAHs based on the Quick Easy Cheap Effective Rugged and Safe (QuEChERS) approach. The optimized method involved extraction by mechanical agitation with acetonitrile (ACN) as solvent, then purification by SPE using SiO_2 as sorbent. The method gave identical results compared to traditional pressurized liquid extraction (PLE), which favors the QuEChERS approach due to reduced extraction cost. Analysis was performed with GC coupled to a mass spectrometer working in NICI mode.

In this study, both particle and gaseous phase nitro- and oxy-PAHs were studied. Sampling was carried out with high volume air sampling, using quartz fiber filters (QFFs) and polyurethane foam (PUF) as sampling media (see Section 2.2). The analytes in particle phase were extracted from the filters by the QuEChERS method adapted from Albinet et al. (2014). The procedure is described in Section 3.3.1. The analytes in gaseous phase were extracted from the PUF by Soxhlet extraction, as reported by Reisen and Arey (2005) and Cochran et al. (2012). The principles of Soxhlet extraction is presented in Section 2.3. Extracts from both extraction methods were purified by SPE, a method presented in Section 2.4. The analyses were carried out by GC/NICI-MS, and the basic principles of the analytical instrument is presented in Section 2.5.

2.2 High volume air sampling

High volume air sampling is an active air sampling method that is typically used to collect volatile and semi-volatile organic pollutants in the atmosphere. Pollutants are collected and concentrated over a period of time to obtain average exposure levels during the entire sampling period. Such systems are used world wide in international monitoring programs of atmospheric pollutants (Hung et al., 2005).

A schematic figure of a high volume air sampler is shown in Figure 2.3. Air is pulled through a dual chambered sampling module by a pump, where suspended airborne particulates are collected on a filter and airborne vapors are trapped in the polyurethane foam (PUF) below. The high volume air samplers used in this study can collect air samples at flow rates up to 16.8 cubic meters per hour (Tisch Environmental Inc. (n.d.)).

It is not possible to determine gas-particle partitioning properties directly by using high volume air samplers. Particle-bound molecules may pass through the filter and be incorrectly assessed as gas phase molecules. On the contrary, gas phase molecules may adsorb to the filter when the filter loadings are low, and be incorrectly assessed as particle-bond molecules (Hart et al., 1992). However, these events are assumed negligible in this study.

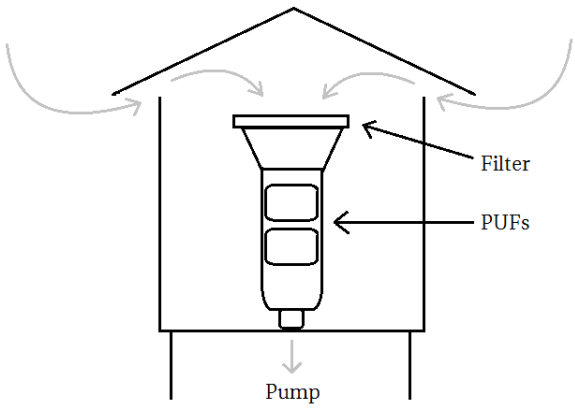

Figure 2.3: Schematic figure of a high volume air sampler. Figure adapted from a lecture slide by H. Hung (lecture in course AT-331 at UNIS, April 18, 2016).

Breakthrough effect can occur for analytes of high volatility and/or high concentrations, and has been reported for three-ring PAHs by Hart et al. (1992). These effects can be investigated by adding a backup layer of sorbent in the sampling module, in this case a second PUF in the bottom of the module. The measure of breakthrough is given by (Hart et al., 1992)

$$B(\%) = \frac{S}{P+S} \cdot 100\% \tag{1}$$

where S is the concentration found in the lower PUF and P is the concentration found in the upper PUF. When B values are less than 20%, $P+S$ will be a good estimate of the total concentration. Breakthrough effect is noteworthy for B values approaching 50%, hence $P+S$ will not be a good estimate of the total concentration (Hart et al., 1992).

2.3 Soxhlet extraction

The Soxhlet extraction system consists of a round bottom flask placed in a heating mantle, with an attached Soxhlet tube and a condenser with cooling water (see Figure 2.4). A proper extraction solvent is added to the round bottom flask together with a couple of boiling stones. When the round bottom flask is gently heated, vapor of solvent passes through the side tube in the Soxhlet and reaches the reflux condenser, where the vapor of solvent condenses and drips into the sampling material that is located in the thimble chamber. When the thimble chamber is full, the solvent drains back into the flask through the siphon device, and thereby extract the analytes from the sample matrix. The cycle repeats for a pre-determined time period. The extracted analytes accumulate in the round bottom flask while the solvent recirculates, as the solvent has a lower boiling point than the analytes (Mitra and Brukh, 2003, p.142).

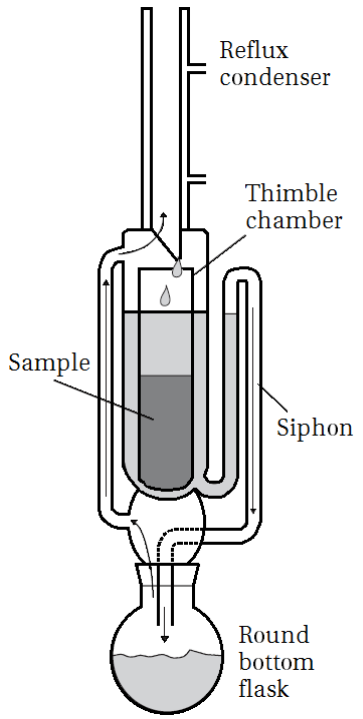

Figure 2.4: Schematic diagram of a Soxhlet extractor (Harvey, 2000, p.214).

2.4 Solid-phase extraction

Solid-phase extraction (SPE) is a sample extraction and purification technique where the sample is passed through a cartridge containing solid material that serves as adsorbent (Harvey, 2000, p.212). Various interactions are used to separate analytes from the matrix and other interfering compounds. The sample is added to a column that contains adsorbent material, and fractions are achieved by elution with solvents of different polarity. The choice of adsorbent material and elution solvents is dependent on the properties of the analytes and matrix (Lundanes, 2014, pp.168-171).

Two general separation procedures by SPE are illustrated in Figure 2.5. In the upper case, the analyte molecules are retained while interfering components are washed from the adsorbent. The analyte molecules are later removed from the adsorbent by elution with a suitable solvent. The lower case shows a procedure where the interfering components are retained while analyte molecules are washed from the adsorbent (Macherey-Nagel (n.d.)).

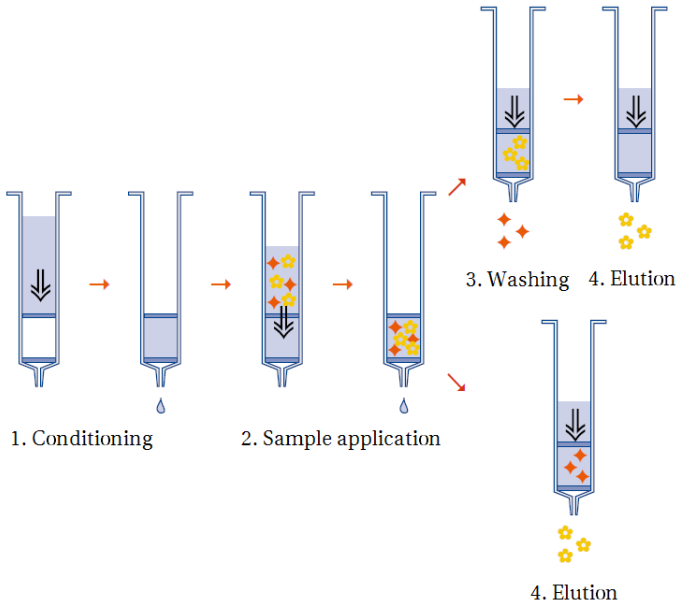

Figure 2.5: Illustration of two general separation procedures by SPE. Figure adapted from Macherey-Nagel (n.d.).

2.5 Gas chromatography/mass spectrometry (GC/MS)

Gas chromatography (GC) is a technique that separates volatile compounds in a sample by carrying the sample with a mobile phase (an inert gas) through a column containing a stationary phase. Separation occurs either by adsorption to a solid stationary phase (gas-solid chromatography, GSC) or by partition between the mobile phase and a liquid stationary phase (gas-liquid chromatography, GLC). The latter is the most frequent method today and is consequently common to refer to as simply GC. The main parts of a gas chromatograph are 1) an injection system, 2) a column contained inside an oven and 3) a detector (Lundanes, 2014, pp. 17-18).

The mass spectrometer is an important detector in gas chromatography. It can provide structural information of compounds, which can be used for identification and quantification of analytes (Lundanes, 2014, pp.32-33). More information about the mass spectrometer is presented in Section 2.5.3.

2.5.1 Injection system

Different sample introduction methods can be used in GC. The most frequent injection system is the split/splitless injector, where splitless injection is required in trace analysis. In splitless injection, the sample is introduced to a heated liner in a hot chamber where the sample evaporates. Then, most of the sample is transferred to the column, which is held at a temperature of the solvent's boiling point with the purpose of condensing the analytes and remove solvent remains. During this time, the solutes concentrate in the column entrance. Separation of the analytes begins when the column temperature increases (Harvey, 2000, p.568).

Pulsed splitless injection was used in this study. This injection technique uses a carrier gas pressure pulse during injection, which makes it possible to increase the injected sample volume up to 5 µL without risks of inlet overflow with sample vapors (Godula et al., 2001). Consequently, lower detection limits can be obtained. Compared to normal splitless injection, this technique has been shown to minimize possible thermal decomposition of analytes in the injection port, as well as improve the transfer of samples into the column (Sasaki and Makino, 2006).

2.5.2 Column

There are two general types of columns in gas chromatographs: packed columns and capillary columns. For most current applications, packed columns have been replaced by capillary columns, as they are faster and more efficient (West et al., 2014, p.890). Wall-coated open tubular columns (WCOT) are by far the most used in gas chromatography (Lundanes, 2014, p.26). The liquid stationary phase is coated as a thin film (typically 0.25 μm) on the inner wall of the capillary. The type and amount of stationary phase influence the retention of the compounds in the column, and have to be chosen on the basis of the analyte properties (Harvey, 2000, p.536).

The column in this study contained a stationary phase of 5% phenyl-substituted methylpolysiloxane, which is a non-polar phase that is frequently used in organic environmental analysis. The column is equivalent to the columns used by Cochran et al. (2012) and Albinet et al. (2014), among others.

2.5.3 Mass spectrometry

The basic principle of mass spectrometry (MS) is to generate charged ions from inorganic or organic compounds by a suitable ionization technique, to separate these ions by their mass-to-charge ratio (m/z) and to detect them qualitatively and quantitatively. Accordingly, a mass spectrometer consists of an ion source, a mass-to-charge separation unit (mass analyzer) and an ion detector, which are operated under high vacuum conditions (Gross, 2004, pp.3-4). The variations of mass spectrometers are many, and the following presents the basic concept of a triple quadrupole mass spectrometer with negative ion chemical ionization (NICI), which was used in this study.

Chemical ionization (CI) is a soft ionization method, which yields in little or no fragmentation of the compounds in the sample. Consequently, this method is important for determination of molecular weight. A schematic layout of a CI ion source is shown in Figure 2.6. In CI, a reagent gas (for instance methane) is present in the ion source, and most of the emitted electrons interact with reagent gas molecules, forming reagent ions. When the sample molecules interact with the reagent gas ions, new ionized species are formed. When negative ion CI is performed, the analyzer voltage is adjusted to select negative ions. CI provides lower detection limits than for instance electron ionization (EI), as the sensitivity for the molecular ion is

high (Gross, 2004, p.331).

The triple quadrupole mass spectrometer consists of an ion source followed by one quadrupole, a collision cell, a second quadrupole and a detector. A quadrupole is a mass analyzer that consists of four parallel hyperbolic rods. The pairs of opposite rods are held at a certain potential, which is composed of a DC (dirrect current) and an AC (alternating current) component. They create an oscillating electric field where selected ions are filtered (Gross, 2004, pp.146-147). The triple quadrupole can be operated in different modes. In this study, the mass spectrometer was operated in selected ion monitoring (SIM) mode, where all quadrupoles were used in series under the same current and lens conditions. In SIM mode, the mass analyzer acquires only the ionic masses of interest, here two characteristic ions for each target compound, which increases the senisitivy compared to full scan mode (Gross, 2004, p.478).

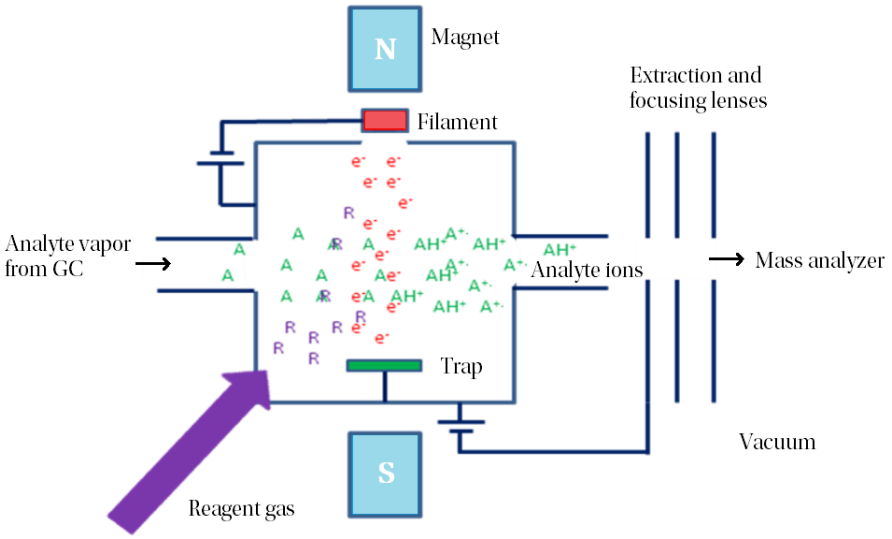

Figure 2.6: A schematic layout of a CI ion source. Figure adapted from (University of Pittsburgh (n.d)).

3 Materials and methods

The field work and most of the laboratory work in this study took place at the University Centre in Svalbard (UNIS) in Longyearbyen, Svalbard, Norway. The samples were analyzed at the Faculty of Chemistry, Biotechnology and Food Science at the Norwegian University of Life Sciences (NMBU) in Ås, Norway.

3.1 Sampling

Twelve high volume air samples were collected in Longyearbyen within a period of six weeks during late winter and early spring 2017 (12/02/17 - 17/03/17). A map of the sampling sites is shown in Figure 3.1. The first week of sampling was carried out on the roof of UNIS (78° 13'21.36"N, 15°39'07.92"E), an urban site centered in Longyearbyen close to the coal power plant and local traffic. The rest of the sampling was carried out in Adventdalen, 5 kilometers outside town, at the old Aurora Station (78°12'09.00"N, 15°49'41.88"E), where the samplers were assembled at the top of a container (see Figure 3.2). This site is further away from the power plant, but is still exposed to emissions from coal trucks, cars and snowmobiles. When the wind direction is from north-west it is also believed that the emissions from the power plant will reach this site.

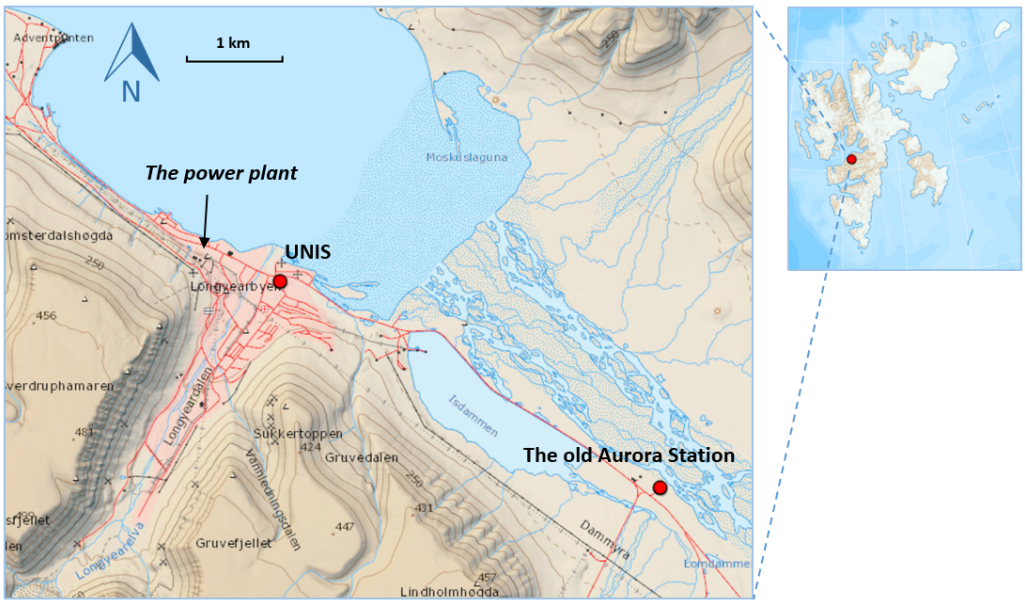

Figure 3.1: Map showing the location of the sampling in Longyearbyen, Svalbard, Norway. The map is created from the online map *Svalbardkartet*, delivered by the Norwegian Polar Institute (2017).

The air samples were collected with TE-1000-BL PUF Poly-Urethane Foam High Volume Air Sampler (Tisch Environmental, Inc., Cleves, OH, USA). Air sampler number 5127 was used for all samples, except sample N10, which was collected with air sampler number 5128. In order to record correct air flow through the samplers, they were calibrated at each site using a calibration orifice, following the calibration procedure stated in the manual from Tisch Environmental Inc. (n.d.). The correlation coefficient for all calibrations fulfilled the requirement of minimum 0.990. The calibration data can be found in Appendix A.3.

The QFFs used for sampling at UNIS were micro-quartz fiber filters from Munktell (103 mm, Ahlstrom Germany GmbH, Nümbrecht, Germany), but because of limited access to these filters, the filters were changed to quartz microfiber filters from Whatman (101.6 mm, GE Healthcare Life Sciences, Maidstone, United Kingdom) for sampling at the old Aurora Station. Each sample consisted of one QFF and two PUFs (D=2.5 inch, L=2 inch, Sunde Søm & Skumplast A/S, Gan, Norge). Prior to sampling, the QFFs were burned at 450 °C for 4 hours, in order to remove potential organic contaminations. They were individually wrapped in aluminum foil and stored in a desiccator at room temperature (25°C). The PUFs were cleaned at the Norwegian Institute of Air Research (NILU, Kjeller, Norway) by Soxhlet extraction with toluene (24 hours), followed by acetone (8 hours) and cyclohexane (8 hours). They were wrapped in aluminum foil, placed in zip lock bags and stored in plastic containers at room temperature.

This study aimed for sampling at days without precipitation, as rapid deposition of particulate matter is likely to occur during precipitation. However, in the end of the sampling campaign, precipitation could not be avoided. The sampling time varied from 24 to 120 hours, and the sample volumes varied from 251 to 2251 m^3. The sampling time was increased throughout the sampling period, because there was a concern that the earlier sample volumes were too small to obtain detectable amounts of nitro- and oxy-PAHs. Details regarding sampling time, sampling volume and weather conditions for each sample is listed in Table A.1 in Appendix A.1. After sampling, each QFF and PUF was wrapped in aluminum foil and placed in double zip lock bags, then stored at -18 °C until sample preparation (maximum three weeks). Nitrile gloves and tweezers were used during handling of samples in order to minimize contamination.

In order to investigate possible contamination during handling, transport and storage, blank

samples were brought to each site and exposed in air without air filtration, before they were stored and extracted in the same way as the other samples.

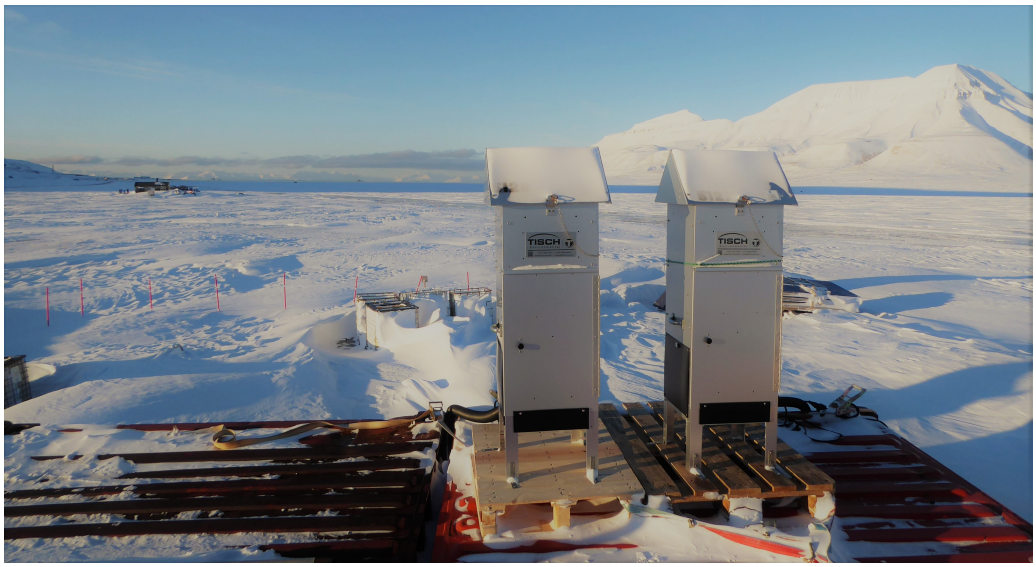

Figure 3.2: Sampling at the old Aurora Station, March 12, 2017.

3.2 Standards, chemicals and materials

A complete list of all standards, chemicals and materials can be found in Appendix B. Standards of nitro- and oxy-PAHs were purchased from CHIRON AS, Trondheim, Norway, and chemicals were purchased from VWR International (Oslo, Norway) and Merck KGaA (Darmstadt, Germany) and were of trace analysis grade.

All equipment used during field and laboratory work was cleaned thoroughly prior to use in order to reduce possible contamination of samples. All glassware was cleaned in a laboratory dishwasher (Ken Hygiene Systems, Broby, Denmark), burned at 450 °C for 8 hours (High-temperature furnace HTC, Nabertherm GmbH, Lilienthal, Germany), and rinsed with the solvent in use. Equipment that is not suitable for burning (e.g. screw caps and tweezers of metal) was cleaned in dishwasher and rinsed with solvents of different polarity.

3.3 Sample Preparation

In order to study the distribution of nitro- and oxy-PAHs between particulate and gaseous phase in the atmosphere, filters and PUFs were extracted separately. A schematic representation of the sample preparation procedure is shown in Figure 3.3.

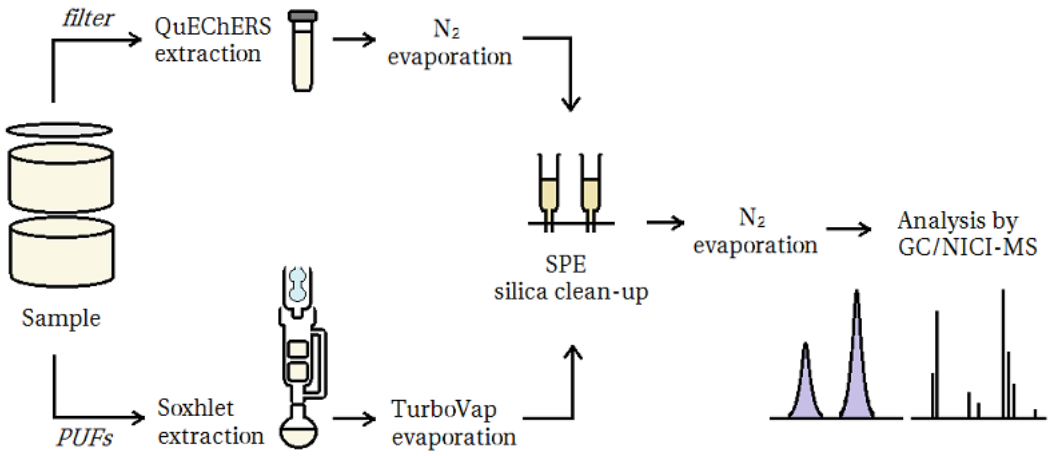

Figure 3.3: A schematic representation of the sample preparation procedure.

3.3.1 Extraction of filters

The method for filter extraction is developed by Albinet et al. (2014) and is based on the QuEChERS approach in extraction of organic contaminants.

The filters were folded and placed in centrifuge test tubes, where 25 ng internal standard mixture (ISTD, 2-nitrobiphenyl-d_9 and 9-fluorenone-d_8) was added onto the filters. Two method blanks (one filter from Munktell (MB1) and one filter from Whatman (MB2)) were spiked with 30 ng nitro- and oxy-PAHs and extracted in parallel with the samples, in order to evaluate the accuracy of the method.

7 mL ACN was added to the test tubes so the filters were totally immersed in solvent. The tubes were then shaken by vortex mixing with a multi-position vortex mixer (VWR International AS, Oslo, Norway) for 2 minutes. Next, samples were centrifuged (Universal 16 R Centrifuge, Nerliens Meszansky AS, Oslo, Norway) for 5 minutes at 4000 rpm (4500 rpm used by Albinet et al. (2014), but 4500 rpm could unfortunately not be achieved in this study, as the maximum speed for the available centrifuge was 4000 rpm). Supernatant (approximately 2 mL) was collected and transferred to new test tubes, and the filter extraction was repeated twice in order to increase the extraction efficiency. For the second and third extraction, it was necessary to refill the centrifuge test tubes with 3 mL ACN in order to immerse the filters again. After the third extraction, the filters were removed from the tubes with tweezers before the extracts were transferred to the tubes holding supernatants from the first and second extraction. The final extract volumes were approximately 10-12 mL.

The extracts were concentrated to near dryness under a gentle nitrogen stream using a 12-position N-EVAP Nitrogen Evaporator (Organomation, Berlin, MA, USA). The stainless steel needles were pre-cleaned with dichloromethane (DCM) in ultrasonic bath (Ultrasonic Cleaner USC600T, VWR International, Leuven, Belgium) for 10 minutes. When the samples were near dryness, the inner walls of the test tubes were rinsed with 1 mL of ACN in case some analytes were stuck to the walls. The samples were again concentrated to near dryness and dissolved in 200 µL DCM.

3.3.2 Extraction of PUFs

All PUFs were extracted by Soxhlet extraction with DCM as extraction solvent. DCM was chosen on the basis of earlier research (Meyer et al., 1999; Reisen and Arey, 2005 Cochran et al., 2012). For most samples, both the upper and lower PUF was added to the same Soxhlet tube and hence extracted together. However, the upper and lower PUF for sample N4, N6, N9 and N10 were extracted separately, in order to investigate breakthrough during sampling. Two method blanks (clean PUFs spiked with 30 ng of nitro- and oxy-PAHs) were extracted in parallel with the samples. 25 ng internal standard mixture was added onto the PUF(s) before the extraction started. 350 mL DCM was added to the round bottom flask, together with three boiling stones (pre-cleaned with DCM in ultrasonic bath for 10 minutes). The Soxhlet extraction was run for eight hours.

Prior to sample clean-up, the extracts were transferred to TurboVap tubes for solvent reduction by TurboVap (TurboVap 500, Caliper Life Sciences, Waltham, MA, USA). In order to minimize loss of analytes, the round bottom flask was rinsed three times with 1 mL of DCM, which was also transferred to the TurboVap tube. The TurboVap system was cleaned in advance by running it with acetone as solvent twice, first with the fan off and then with the fan on. The temperature in the water bath was set to 35 °C. The sample extracts were evaporated until the solvent reached the sensor endpoint, which was 0.5 mL. The inner walls of the TurboVap tube was rinsed three times with DCM, and the volume was again reduced to 0.5 mL. Then, the sample was transferred to an amber vial, and the TurboVap tube was again rinsed three times with some droplets of DCM, which was also transferred to the sample vial.

3.3.3 Sample clean-up

The extracts from the filter extraction and the PUF extraction followed the same clean-up procedure. The clean-up procedure is a part of the QuEChERS extraction method developed by Albinet et al. (2014), and is done by solid phase extraction (SPE), in order to remove interfering compounds such as alkanes and remnants of matrix. The SPE system used in this study was a CHROMABOND vacuum manifold with SiOH cartridges (Macherey-Nagel, Düren, Germany), connected to a vacuum flask and a vacuum pump.

First, the SiOH cartridges were conditioned with pentane. The sample extracts were added to the columns, and 1 mL pentane was discarded for the removal of alkanes. Then, the sam-

ples were eluted with 9 mL 35:65 (*v/v*) DCM-pentane. The samples were again concentrated to near dryness by nitrogen evaporation (same procedure as the concentration of filter extracts as described in Section 3.3.1). When the samples were near dryness, they were dissolved in 500 µL cyclohexane. The samples were transferred to amber sample vials, and the vials were transported to NMBU for further volume reduction and analysis.

At NMBU, the volume of the samples were reduced to 150 µL under a gentle stream of nitrogen. The stainless steel needles were cleaned with acetone in ultrasonic bath for 10 minutes. The samples were transferred to sample vials with insert, and 25 ng recovery standard (RSTD, fluoranthene-d_{10}) was added to each sample.

3.4 Preparation of calibration standards

A 1 ng mL^{-1} stock solution of 21 nitro-PAHs and 11 oxy-PAHs was prepared by dilution and mixing of single compound standard solutions (listed in Table B.1). Calibration standards of approximately 25, 50, 100, 200, 300 and 500 pg μL^{-1} were prepared by dilution of the stock solution with cyclohexane. A constant amount of ISTD (100 pg μL^{-1}) and RSTD (100 pg μL^{-1}) was also added to each calibration standard solution.

Calibration standards containing a constant amount of RSTD (100 pg μL^{-1}) and varying concentration of ISTD (25, 50, 100, 200, 300 and 500 pg μL^{-1}) were also prepared, in order to establish a relationship between the ISTDs and RSTD with the purpose of determination of recovery.

3.5 Instrumental analysis

The analyses were carried out using an Agilent 7890B GC-system coupled to a 7000C Triple Quadrupole Mass Spectrometer with NICI ion source (Agilent Technologies, Santa Clara, USA). The column was a 5% phenyl-substituted methylpolysiloxane (HP-5ms, 30m x 0.25 mm, 0.25 µm film thickness, J&W Scientific, Agilent Technologies, Santa Clara, USA).

The conditions for the GC/NICI-MS analyses were determined from Albinet et al. (2014) and earlier work within the analysis of nitro- and oxy-PAHs by GC/NICI-MS conducted at the faculty. The conditions are listed in Table 3.1 and details on equipment is given in Appendix B.3. Retention times and monitored ions in SIM mode for each target compound and ISTD/RSTD

are listed in Table 3.2.

Before the analyses of the calibration standards and samples, a standard solution of 1000 pg μL^{-1} was analyzed in full scan mode in order to verify the retention times and monitored ions for each target compound, previously determined by Garstad (2016). Three target compounds were not detected in full scan mode, and were therefore excluded from the study. These compounds were 4H-cyclopenta[*d,e,f*]phenanthren-4-one, 2-methyl-9,10-anthraquinone and 9-methylcarbazole.

Every calibration standard and sample was run twice, and blank samples (pure *n*-hexane) were analyzed after every third sample in order to check for carry-over effects. A standard solution of 100 pg μL^{-1} nitro- and oxy-PAHs was analyzed after every tenth sample in order to monitor possible changes in analyte response throughout the sample sequence.

Chromatograms were processed by the computer software "Agilent MassHunter Qualitative Analysis B.07.00" and "Agilent MassHunter Quantitative Analysis B.07.01". The first program was used for confirmation of retention times and qualifier/quantifier ions, while the latter was used for integration of peaks. Peaks were mostly integrated automatically by the algorithm "Agile2", but some peak areas had to be adjusted manually due to peak asymmetry. Signal-to-noise ratio (S/N) was calculated by MassHunter by the algorithm "ASTM" with a noise standard deviation multiplier of 5. The data was exported to Microsoft Excel 2013 where the quantification was carried out.

Table 3.1: Conditions for the GC/NICI-MS analyses.

Parameter	Value
Injection system	
Injection mode	Pulsed splitless
Pulse pressure	25 psi until 0.75 min
Injection volume	2 µL
Temperature	250 °C
Septum purge flow	3 mL/min
Purge flow to split vent	50 mL/min at 2 min
Syringe washing solvent	*n*-Hexane
Column	
Stationary phase	5% phenyl-methylpolysiloxane (HP-5ms)
Carrier gas	Helium (6.0)
Flow	1 mL/min
Initial temperature	70 °C
Temperature program	70 °C for 2 min
	15 °C/min to 180 °C
	5 °C/min to 280 °C, hold for 5 min
	15 °C/min to 325 °C, hold for 5 min
Total program time	42.33 min
Mass spectrometer	
Mass spectrometer type	Triple quadrupole
Ionization technique	Negative ion chemical Ionization (NICI)
Methane flow rate	2 mL/min
Quench gas	He, 2.25 mL/min
	N_2, 1.5 mL
Transfer line temperature	300 °C
Ion source temperature	200 °C
Emission current	50 µA
Electron energy	135 eV
Tuning	Auto tune
Electron energy mode	Use tune setting
Solvent delay	3.75 min
Stop time	42 min
Scan mode	MS1 SIM (monitored ions listed in Table 3.2)
Dwell time	25 ms

Table 3.2: Overview of the target compounds and the internal standards (in italics) and recovery standard (in italics), their corresponding characteristic ions, peak number and retention time.

Compound	Peak no.	Retention time [min]	Quantifier ion [*m/z*]	Qualifier ion [*m/z*]
Nitro-PAHs				
2-Nitrobiphenyl-d_9	*4*	*11.38*	*208*	*209*
1-Nitronaphthalene	2	10.55	173	174
2-Nitronaphthalene	3	10.94	173	174
4-Nitrobiphenyl	7	13.23	199	200
5-Nitroacenaphthene	10	15.32	199	200
2-Nitrofluorene	12	16.67	211	212
9-Nitroanthracene	13	17.14	223	224
9-Nitrophenanthrene	14	18.17	223	224
2-Nitroanthracene	16	19.49	223	224
2-Nitrofluoranthene	19	22.97	247	248
3-Nitrofluoranthene	20	23.03	247	246
4-Nitropyrene	21	23.26	247	248
1-Nitropyrene	23	23.82	247	248
2-Nitropyrene	24	24.13	247	248
2,7-Dinitrofluorene	25	24.74	256	257
7-Nitrobenz[*a*]anthracene	26	26.63	273	274
6-Nitrochrysene	28	27.81	273	257
1,3-Dinitropyrene	29	28.93	292	276
1,6-Dinitropyrene	30	29.68	292	293
1,8-Dinitropyrene	31	30.25	292	276
6-Nitrobenzo[*a*]pyrene	-	34.03	297	298
Oxy-PAHs				
9-Fluorenone-d_8	*5*	*11.89*	*188*	*189*
1,4-Naphthoquinone	1	8.77	158	159
9-Fluorenone	6	11.92	180	181
1-Indanone	8	13.32	148	149
9,10-Anthraquinone	9	14.77	208	209
9,10-Phenanthrenequinone	15	18.60	208	209
Benzo[*a*]fluoren-11-one	17	20.19	230	231
Benzanthrone	18	22.24	230	231
1,2-Benz[*a*]anthraquinone	22	23.62	258	259
6H-Benzo[*c,d*]pyren-6-one	27	27.17	255	254
Recovery standard				
Fluoranthene-d_{10}	*11*	*15.96*	*212*	*213*

3.6 Identification of analytes

According to Oehme (2007, p.19), there are three criteria that are most frequently applied in order to confirm the identity of a given target compound in chromatography. First, the retention time should be within a specified time frame compared to an internal standard or an external standard solution. Secondly, the response should be above a detection limit based on a minimal signal-to-noise ratio. The third criteria is related to simultaneous presence of given characteristic ions (quantifier and qualifier ions) when mass spectrometry is the detector in use. This is defined as the qualifier response ratio, QRR, and is calculated from the peak area of the quantifier and qualifier ion:

$$QRR = \frac{A_{\text{qualifier}}}{A_{\text{quantifier}}} \cdot 100 \tag{2}$$

In this study, the retention times were determined by analysis of a standard solution containing all target compounds. The qualifier response ratio for every compound was determined as the average from the calibration standards. The limit of detection (LOD) was determined for each compound from the three lowest calibration standards (see Section 3.6.1). Identification of each analyte was confirmed when the retention time was within 0.1 minutes, the qualifier response ratio was within 20% and the analyte response was above the LOD.

3.6.1 Limit of detection

The LOD was calculated from the calibration curve of every compound given by the following equations (Harris, 2010, pp.103-105):

$$LOD \ \text{[pg/µL]} = 3 \cdot \frac{s_y}{m} \tag{3}$$

$$LOD \ \text{[pg]} = LOD \ \text{[pg/µL]} \cdot 2 \ \text{µL}$$

where m is the slope of the calibration curve and s_y is the standard error of the predicted y-value for each x-value obtained by least square linear regression. The LOD was multiplied by two because of the injection volume of 2 µL. The three lowest calibration standards were used for the determination of LOD (six data points in total).

For some compounds, it was not possible to construct calibration curves, because the re-

sponse was too low for the lower calibration standards (see in Section 4.2). Here, the LOD was estimated from the signal-to-noise ratio of the calibration standards where the analyte response was acceptable (mostly the calibration standards of 300 and 500 pg μL^{-1}). The signal corresponding to the LOD, S_{LOD} is given as (Lundanes, 2014, p.190)

$$S_{LOD} = 3 \cdot \frac{S_i}{N} \tag{4}$$

where S_i is the height of the analyte peak and N is the height of the noise band. Furthermore, the concentration of the LOD, C_{LOD}, was found using the following relationship:

$$\frac{C_{LOD}}{S_{LOD}} = \frac{C_i}{S_i} \tag{5}$$

where C_i is the concentration of the analyte in the standard solution. The reported C_{LOD} value for the compounds in question was the average value from the calibration standards that were included in the calculations.

3.7 Quantification of analytes

Analytes were quantified by the internal standard method, which is a commonly used method for quantification in chromatographic analyses. An internal standard is a deuterium labelled/ non native compound of similar chemical properties as the analyte, which is added to the sample prior to sample preparation. In this study, one deuterated nitro-PAH was used as ISTD for the nitro-PAHs (2-nitrobiphenyl-d_9) and one deuterated oxy-PAH was used as ISTD for the oxy-PAHs (9-fluorenone$_8$). The advantages of the internal standard method are that it compensates for sample losses which occur during sample preparation and analysis, and also compensates for variations in injected sample volume (Poole, 2003, pp.65-71). In addition, it is not necessary to know the final sample volume, and evaporation of small amounts of solvent does not influence the quantification (Oehme, 2007, p.25).

Calibration curves were established by analyzing six standard solutions of varying concentrations of nitro- and oxy-PAHs (approximately 25-500 pg μL^{-1}), as well as a constant concentration of ISTD (100 pg μL^{-1}) and RSTD (100 pg μL^{-1}). A calibration curve was constructed for each target analyte by plotting the ratio of analyte concentration and ISTD concentration (x) against the ratio of analyte response and ISTD response (y).

In other words, each calibration curve was given by

$$y = mx + b \tag{6}$$

where m and b are constants determined from least square linear regression in Microsoft Excel. The amount of analyte in every sample was furthermore calculated by rearrangement of Equation 6:

$$M_i \ \text{[ng]} = \frac{M_{ISTD}}{m} \cdot \left(\frac{A_i}{A_{ISTD}} - b \right) \tag{7}$$

where M_{ISTD} is the amount of ISTD that was added to the sample before sample preparation. Finally, the concentration of the different nitro- and oxy-PAHs in the sampled air volume (V_{air}) was calculated by

$$C_i \ \text{[pg/m}^3\text{]} = \frac{M_i}{V_{air}} \cdot \frac{1000 \text{ pg}}{\text{ng}} \tag{8}$$

3.7.1 Limit of quantification

Similar to the LOD, the limit of quantification (LOQ) was determined from the calibration curve of every compound given by (Harris, 2010, p.103-105)

$$LOQ \ \text{[pg/µL]} = 10 \cdot \frac{s_y}{m} \tag{9}$$

$$LOQ \ \text{[pg]} = LOQ \ \text{[pg/µL]} \cdot 2 \ \text{µL}$$

where m is the slope of the calibration curve and s_y is the standard error of the predicted y-value for each x-value obtained by least square linear regression. The LOQ was multiplied by two because of the injection volume of 2 µL. As for LOD, only the three lowest calibration standards were used for the determination of LOQ (six data points in total).

3.7.2 Recovery

The loss of analytes during extraction and clean-up was determined from the response factor (f_r) of the internal standards relative to the recovery standard, which is given by the following equation (Oehme, 2007, p.25):

$$f_r = \frac{C_{ISTD} \cdot A_{RSTD}}{C_{RSTD} \cdot A_{ISTD}} \tag{10}$$

where C_{ISTD} and C_{RSTD} are the concentrations of the internal standard and the recovery standard in the standard solution and A_{ISTD} and A_{RSTD} are the peak areas of the internal standard and the recovery standard in the chromatogram of the standard solution. f_r was calculated for each of the six calibration standards (with ISTD concentration from 25 to 500 pg μL^{-1}), and the average value was used in the calculation of recovery.

The recovery, R, in every sample is further given by (Oehme, 2007, p.25):

$$R\ [\%] = \frac{M_{RSTD} \cdot A_{ISTD} \cdot f_{r,avg} \cdot 100\%}{M_{ISTD} \cdot A_{RSTD}} \tag{11}$$

where M_{ISTD} and M_{RSTD} are the amounts of internal standard and recovery standard added to the sample and A_{ISTD} and A_{RSTD} are the peak areas of the internal standard and recovery standard in the chromatogram of the sample. The recovery was calculated for both 2-nitrobiphenyl-d_9 and 9-fluorenone-$_8$ for every filter and PUF sample.

3.7.3 Accuracy

Accuracy is defined as the deviation from the true value (Mitra and Brukh, 2003, p.6). The deviation between the spiked and determined levels of nitro- and oxy-PAHs in the spiked method blanks was calculated from:

$$E(\%) = \frac{|\text{Determined amount} - \text{Spiked amount}|}{|\text{Spiked amount}|} \cdot 100\% \tag{12}$$

3.7.4 Precision

Precision is a measure of repeatability and is affected by random errors, which occur in all measurements (Harvey, 2000, p.62). In the process of quantification, an arithmetic mean ($\bar{x}$ from repeated measurements was reported as the final concentration, which is given as (Mitra and Brukh, 2003, p.7):

$$\bar{x} = \frac{\Sigma x_i}{n} \tag{13}$$

where Σx_i is the sum of the replicate measurements and n is the total number of measurements. The random errors are assumed to be normally distributed, and the standard deviation (s) is calculated as:

$$s = \sqrt{\frac{\Sigma(x_i - \bar{x})^2}{n-1}} \tag{14}$$

4 Results and discussion

4.1 GC/NICI-MS analysis

The analytical method made it possible to identify 28 out of 32 nitro- and oxy-PAHs in SIM mode. A typical total ion chromatogram of a standard solution containing all target compounds is shown in Figure 4.1. The corresponding compound to each peak number can be found in Table 3.2.

The target compounds that could not be identified were 4H-cyclopenta[*d,e,f*]phenanthren-4-one, 2-methyl-9,10-anthraquinone, 9-methylcarbazole and 6-nitrobenzo[*a*]pyrene. The three first compounds could not be detected in full scan mode of a standard solution and were therefore not investigated further in the study. The latter compound was not identified due to low sensitivity of late eluting peaks. In addition, reliable identification of 1-indanone could not be carried out, as there was high presence of this compound in the analysis of blanks (pure *n*-hexane). Accordingly, identification could be carried out for 27 target compounds (19 nitro-PAHs and 8 oxy-PAHs).

One of the major issues during the chromatographic analyses was high band broadening, which can be seen in the chromatogram in Figure 4.1. This caused problems for identification and quantification of late eluting compounds, as sensitivity decreased and asymmetry increased with increasing retention time. Solutions for less band broadening might be to lower the GC oven start temperature, increase the temperature rates or increase the flow rates (Restek Corporation, 2013).

Tailing was observed for late eluting compounds, especially in analyses of low concentration standards. Tailing may occur from solute adsorption in the liner or column, thus replacement of these parts could be a solution for less tailing (Restek Corporation, 2013). Another solution for improvement of late eluting peaks could be to increase the transfer line temperature in the interface between the GC and MS. It is recommended to use a higher temperature in the transfer line than the maximum oven temperature (Kelly and Parnell, 2017), which was not the case in the analytical method in this study. A lower transfer line temperature may cause the analytes to condense or slow down and result broad or tailing peaks.

The absence of three of the target compounds in the full scan analysis of a standard solution might result from thermal degradation of the compounds during the GC injection. Albinet et al. (2014) investigated the effect of injection temperature between 110 and 280°C. The responses to nitro- and oxy-PAHs were quite similar between 140 and 200°C, except for dinitropyrene isomers. Albinet et al. (2014) kept the injection temperature at 140°C in the optimized method to prevent possible thermal degradation of nitro- and oxy-PAHs and obtain the highest sensitivity for dinitropyrene isomers. In this study, the temperature was set to 250°C, based on earlier analyses done at the faculty. This is probably not an optimal injection temperature for nitro- and oxy-PAHs in terms of thermal degradation and sensitivity.

As a part of the quality control, blanks (pure *n*-hexane) were analyzed after every third sample in order to check for carry-over effects and contaminations. As already mentioned, 1-indanone was present in blank samples, but all blanks were clean from other target compounds. Hence, it was not necessary to analyze blank samples so frequently, and this could have been adjusted in order to reduce costs. The response check throughout the sample sequence with frequent analyses of a 100 pg μL^{-1} standard solution showed little variation in response.

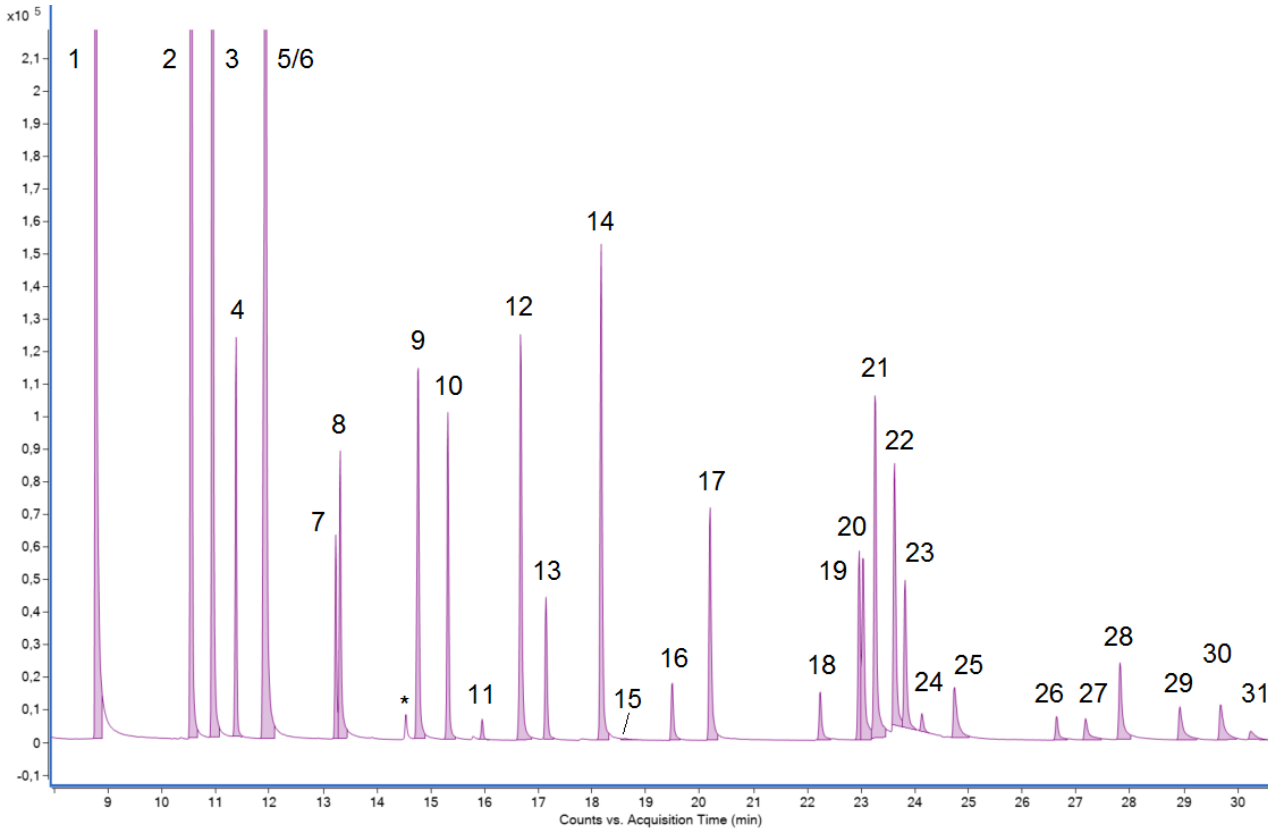

Figure 4.1: GC/MS total ion chromatogram obtained from a standard solution of nitro- and oxy-PAHs (500 pg μL^{-1}, 2 µL injected, SIM acquisition mode). The peak numbers with the corresponding compounds are listed in Table 3.2. Note: peak 1, 2, 3 and 5/6 are cut in order to give better visibility of the late eluting peaks. The peak marked with * is from an impurity in the system.

4.2 Calibration parameters

Calibration curves were established for 19 out of 27 identified compounds. The calibration parameters for each compound that was possible to quantify are listed in Table 4.1, and the calibration curves are presented in Figure C.1-C.19 in Appendix C. For compounds that eluted after 19 minutes, one or more of the lowest calibration standards had to be excluded from the calibration curves as their peaks were too small or asymmetric for integration. This can be seen in the column showing the linear range for each compound in Table 4.1. In contrast, the highest calibration standard was excluded in the calibration curve for 9-nitroanthracene in order to improve the correlation coefficient. The calibration curves for 2-nitropyrene and 7-nitrobenz[*a*]anthracene were based on only three calibration levels. Consequently, the linear regression curve was questionable for these compounds as four or five levels are often recommended as a minimum for linear regression (Hubert et al., 1999).

Due to low sensitivity of the late eluting compounds, calibration curves could not be established for 9,10-phenanthrenequinone, 2,7-dinitrofluorene, 6H-benzo[*c,d*]pyren-6-one and the isomers 1,3-dinitropyrene, 1,6-dinitropyrene and 1,8-dinitropyrene. 2- and 3-nitrofluoranthene were not quantified either, as their separation was poor (peak 19 and 20 in Figure 4.1). However, as already stated by Albinet et al. (2006), their co-elution has to be accepted when the HP-5ms/DB-5ms column is in use. In retrospect, it was discovered that earlier research on levels of nitro-PAHs reported joint concentrations of 2- and 3-nitrofluoranthene, which could have been done in this study as well. On the other hand, none of them were detected in the air samples from Longyearbyen, thus no calibration curve was established for 2- and 3-nitrofluoranthene.

As mentioned in Section 4.1, tailing was observed for low analyte concentrations of late eluting compounds. This will affect the linearity of the calibration curves, as the integration of peaks of low analyte concentrations will be overestimated. In fact, it can be seen in Table 4.1, that the correlation coefficient, decreased with increasing retention time. However, every compound had a correlation coefficient above the threshold value, which was set to 0.95 in this method.

The calibration curves were constructed from the analyses of standard solutions without sample matrix. Poole (2003, p.186) states that this results in an overestimate of the analyte concentration in real samples. Pulsed splitless injection reduces this problem, due to shorter res-

idence time of the sample in the vaporization chamber, which minimizes interactions with active sites. However, as discussed in Section 4.5, analyte concentrations were still overestimated. Nevertheless, it would be expensive and time consuming to make calibration standards containing sample matrix, thus this procedure is not common.

Table 4.1: Calibration parameters used for quantification of the compounds that were possible to quantify in this method, including the calculated LOD and LOQ, given in injected amount in the GC.

Compound	Linear range [pg μL^{-1}]	R^2	m	b	LOD [pg]	LOQ [pg]
1,4-Naphtoquinone	17-322	0.9960	1.5657	0.0048	12.2	40.5
1-Nitronaphthalene	25-472	0.9985	1.4779	-0.1804	3.4	11.2
2-Nitronaphthalene	25-471	0.9978	1.0404	-0.1493	4.7	11.2
9-Fluorenone	18-345	0.9984	1.3622	-0.0961	5.0	16.8
4-Nitrobiphenyl	24-466	0.9969	0.1097	-0.0201	10.7	35.7
9,10-Anthraquinone	21-406	0.9978	0.2191	-0.0316	11.5	38.4
5-Nitroacenaphthene	23-442	0.9968	0.2080	-0.0396	4.9	16.3
2-Nitrofluorene	25-474	0.9945	0.2740	-0.0789	7.1	23.5
9-Nitroanthracene	25-290	0.9859	0.0684	-0.0162	38.8	129.2
9-Nitrophenanthrene	21-410	0.9961	0.3667	-0.0803	18.5	61.8
2-Nitroanthracene	97-471	0.9918	0.0491	-0.0320	68.4	228.1
Benzo[*a*]fluoren-11-one	43-423	0.9926	0.2081	-0.0764	28.2	93.9
Benzanthrone	84-409	0.9803	0.0533	-0.0363	88.9	296.2
4-Nitropyrene	25-474	0.9857	0.2422	-0.1103	24.8	82.5
1,2-Benz[*a*]anthraquinone	41-410	0.9914	0.2819	-0.0998	37.1	123.7
1-Nitropyrene	48-473	0.9807	0.1274	-0.0863	47.2	157.4
2-Nitropyrene[a]	194-475	0.9875	0.0171	-0.0212	93.9	313.1
7-Nitrobenz[*a*]anthracene[a]	192-469	0.9793	0.0292	-0.0423	130.5	435.0
6-Nitrochrysene	97-472	0.9932	0.0861	-0.0655	98.7	328.9

[a] Only three calibration levels used, linear regression questionable

4.3 LOD and LOQ

The LOD and LOQ for the compounds that were quantified are presented along with the calibration parameters in Table 4.1. The LOD for the compounds that could not be quantified, hence calculated by signal-to-noise ratio, is presented in Table 4.2.

As already discussed, high band broadening caused problems for the sensitivity of the late eluting compounds, and this is also reflected by the values of LOD and LOQ. LODs fall in the range of 3.4-1374 pg for nitro-PAHs and of 12.2-288 pg for oxy-PAHs, while LOQs fall in the range of 11.2-435.0 pg for nitro-PAHs and 16.8-296.2 pg for oxy-PAHs. The late eluting com-

pounds had the highest values of LOD and LOQ.

Compared to literature, Albinet et al. (2006) reported LODs and LOQs significantly lower than here, but based their calculations on the signal-to-noise ratio. Cochran et al. (2012) calculated LODs from the calibration curves as in this study, and reported values in the same range as here, although slightly lower and less varied between the early and late eluting compounds.

Improvements that can reduce band broadening (mentioned in Section 4.1) are believed to give lower LODs and LOQs for late eluting peaks.

Table 4.2: Limit of detection for compounds that was not quantified, hence calculated by signal-to-noise ratio. Values are given in injected amount in the GC [pg].

Compound	LOD
6H-Benzo[*c,d*]pyren-6-one	288
2,7-Dinitrofluorene	474
1,3-Dinitropyrene	714
1,6-Dinitropyrene	1374
1,8-Dinitropyrene	600
2-Nitrofluoranthene	100
3-Nitrofluoranthene	600

4.4 Recovery

The recoveries of the internal standards throughout the sample preparation and analyses are illustrated in Figure 4.2 for the a) filter and b) PUF samples, respectively. There was a large difference in the recovery of the filter and PUF samples, where the filter samples had an average recovery of 55% and the PUF samples had an average recovery of 115%. The recovery of 9-fluorenone-d_8 was slightly lower than the recovery of 2-nitrobiphenyl-d_9 for all samples, but the trend was the same for both compounds.

The average recovery of 2-nitrobiphenyl-d_9 obtained in the QuEChERS approach corresponded to the recovery reported by Albinet et al. (2014) (about 50%). Recoveries obtained in Soxhlet extraction were mostly above 100%, which might indicate that this method results in matrix effects that may cause overestimation of analyte concentrations.

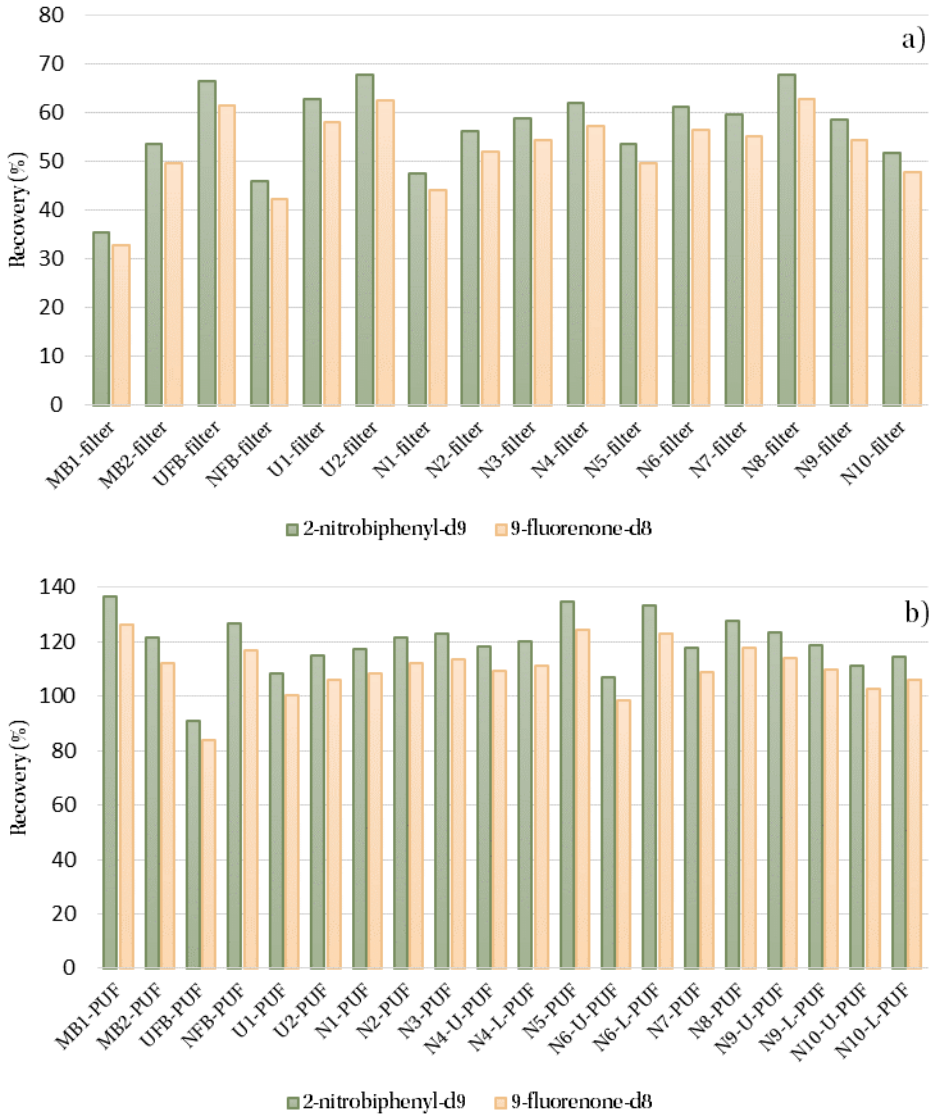

Figure 4.2: Recovery of the internal standards in a) filter samples and b) PUF samples.

4.5 Results from spiked method blanks

As a part of the method validation, four method blanks (MB1-filter, MB2-filter, MB1-PUF and MB2-PUF) spiked with nitro- and oxy-PAH standard solution were prepared and analyzed in parallel with the samples. The method blanks were not spiked with 2-nitrofluorene and 1-nitropyrene as these standards were not available at UNIS.

Table 4.3 presents the determined amounts of nitro- and oxy-PAHs in the method blanks, together with the spiked amount and the percent deviation between the determined and spiked amount (accuracy). The table contains the 19 compounds that were possible to quantify in this method. As can be seen in Table 4.3, the deviation varied from zero to several thousand for individual compounds.

Surprisingly, no clear correlation was found between analyte retention time and accuracy. Although there is a tendency of higher deviations at higher retention times, some of the late eluting compounds showed highest accuracy, such as 4-nitropyrene and 6-nitrochrysene. This illustrates that band broadening may not be the major cause for inaccuracy.

As it can be noted, PUF samples showed higher accuracy than filter samples for all compounds except 2-nitroanthracene. The overestimation of analytes is higher in the filter samples than in the PUF samples. This may result from higher loss of internal standards in the QuEChERS extraction than the Soxhlet extraction, as shown in Figure 4.2. In fact, benzo[*a*]fluoren-11-one and 1,2-benz[*a*]anthraquinone could not be determined in MB1 filter, because the response of the ISTD, 9-fluorenone-d_8, was poor. The recovery was higher in MB2 filter, which explains why the accuracy was higher in this sample compared to MB1 filter. However, the quantification of benzo[*a*]fluoren-11-one and 1,2-benz[*a*]anthraquinone was still highly inaccurate.

Earlier research has shown that 9,10-phenanthrenquinone can be converted into 9-fluorenone by thermal degradation during the GC injection, leading to an overestimation of 9-fluorenone and an underestimation of 9,10-phenanthrenequinone (Liu et al., 2006; Sklorz et al., 2007). This might be the reason why quantification could not be carried out for 9,10-phenanthrenequinone and could explain why 9-fluorenone was overestimated in the filter samples. However, this finding is not in agreement with the results from the PUF samples, where 9-fluorenone is underestimated. Therefore, inaccurate quantification of 9-fluorenone in the filter samples

Table 4.3: Results from spiked method blanks presented with the deviation (dev.) from the added amount before sample preparation.

Compound	M (spiked)	MB1 filter		MB2 filter		MB1 PUF		MB2 PUF	
		M (det.) [a]	Dev.	M (det.)	Dev.	M (det.)	Dev.	M (det.)	Dev.
	[ng]	[ng]	[%]	[ng]	[%]	[ng]	[%]	[ng]	[%]
1,4-Naphthoquinone	28.8	n.d. [b]	-	n.d.	-	n.d.	-	n.d.	-
1-Nitronaphthalene	31.0	19.0 (0.1) [c]	-39	21.5 (0.1)	-30	22.9 (0.1)	-26	26.5 (0.2)	-14
2-Nitronaphthalene	31.2	22.6 (0.1)	-28	23.2 (0.1)	-26	25.1 (0.1)	-20	28.3 (0.5)	-10
9-Fluorenone	29.3	96.0 (-) [d]	228	59.7 (-)	104	22.7 (0.0)	-22	22.0 (0.0)	-25
4-Nitrobiphenyl	31.2	39.9 (0.7)	28	34.6 (0.6)	11	35.7 (0.3)	14	38.7 (1.6)	24
9,10-Anthraquinone	29.9	151.3 (-)	407	98.4 (2.2)	230	15.2 (0.5)	-49	31.8 (0.0)	7
5-Nitroacenaphthene	31.1	43.0 (1.6)	38	34.3 (0.4)	10	35.6 (0.9)	14	37.7 (1.2)	21
2-Nitrofluorene	0	n.d.	-	n.d.	-	n.d.	-	n.d.	-
9-Nitroanthracene	31.0	93.3 (1.0)	201	69.0 (1.3)	123	49.1 (0.1)	59	42.2 (0.2)	36
9-Nitrophenanthrene	30.4	55.5 (2.4)	82	47.9 (0.2)	57	46.0 (0.2)	51	50.1 (1.7)	65
2-Nitroanthracene	30.6	43.8 (3.9)	43	38.2 (0.2)	25	44.1 (0.4)	44	45.3 (0.7)	48
Benzo(a)fluoren-11-one	29.0	n.q. [e]	-	778.2 (-)	2587	57.4 (0.3)	98	45.4 (0.7)	57
Benzanthrone	29.6	n.d.	-	n.d.	-	n.d.	-	20.3 (0.5)	-32
4-Nitropyrene	31.0	36.6 (3.1)	18	33.0 (0.6)	6	31.0 (0.0)	0	33.3 (0.4)	7
1,2-Benz[*a*]anthraquinone	29.8	n.q.	-	2852.1 (-)	9465	177.5 (3.9)	495	161.1 (0.4)	440
1-Nitropyrene	0	n.d.	-	n.d.	-	n.d.	-	n.d.	-
2-Nitropyrene	31.4	n.d.	-	n.d.	-	58.5 (0.4)	87	61.5 (0.7)	96
7-Nitrobenz[*a*]anthracene	31.1	76.9 (9.1)	147	73.2 (2.6)	135	61.8 (1.0)	99	65.3 (1.9)	110
6-Nitrochrysene	30.6	39.8 (3.0)	30	32.8 (-)	7	30.2 (2.0)	-2	34.8 (-)	14

[a] M (det.) denotes determined amount in sample
[b] n.d. denotes not detected
[c] Mean amount (standard deviation)
[d] Only detected in one parallel, standard deviation not calculated
[e] n.q. denotes not quantified, the response of the ISTD was poor

may be more likely to result from low recovery of the ISTD.

1,4-Naphthoquinone was not detected in any method blanks, which means that the compound was lost somewhere in the sample preparation. Most likely, this would origin from the sample clean-up, as this a common step for both filter and PUF samples. At the other hand, Albinet et al. (2014) did not report any particular loss of 1,4-naphthoquinone during the QuEChERS procedure, including clean-up with SPE. Therefore, the absence of 1,4-naphthoquinone is believed to originate from flaws in the standard solution. The method blanks were spiked with standard solutions stored at UNIS, while the calibration standards were prepared from newly purchased standards at NMBU, which means that the standards could be of different quality.

Regarding the compounds that could be identified, but not quantified in this method, only 2-nitrofluoranthene and 3-nitrofluoranthene were detected in the method blanks. The compounds that were not detected were 6H-benzo[*c*,*d*]pyren-6-one, 9,10-phenanthrenequinone, 2,7-dinitrofluorene and the isomers of dinitropyrene, even though the method blanks were spiked with approximately 30 ng of each compound. As previously mentioned, 9,10-phenanthrenequinone might degrade to 9-fluorenone during sampling and analysis. The isomers of dinitropyrene are very difficult to analyze because of their low response (Albinet et al., 2014). The absence of the remaining compounds might be due to flaws in the standard solutions. In retrospect, the standard solutions from UNIS should have been analyzed at NMBU in order to verify their content, in case some of the analytes degrade during storage.

4.6 Levels in air samples from Longyearbyen

Nine of the target compounds in this study were detected and quantified in air samples from Longyearbyen. The compounds not detected is reported as below LOD, which is presented for each compound in Table 4.1 and 4.2. Table 4.5, 4.6 and 4.7 present the average nitro- and oxy-PAH concentrations measured in every sample. The first letter in the sample ID represents the sampling site, where U denotes the roof of UNIS and N denotes the old Aurora Station. FB denotes field blank. U- and L-PUF denotes upper and lower PUF, respectively. All reported levels were above the calculated LOQ, but many compounds had a response below the lowest calibration standard, consequently the quantification can be regarded as semi-quantitative. These values are presented in italics. The values in bold are values within the linear range of the calibration curve.

As it can be noted, the individual concentrations of nitro- and oxy-PAHs were approximately in the same order of magnitude. The exception was 9-fluorenone, which was the most abundant compound and the only compound detected in every sample. For some samples, the concentration of 9-fluorenone was one order of magnitude higher than the remaining compounds. This compound accounted for 43-80% of the total nitro- and oxy-PAH concentration. Other research on air concentrations of nitro- and oxy-PAHs report 9-fluorenone as a dominant compound as well (Albinet et al., 2007; Albinet et al., 2008).

Considering the results from the method blanks, 1- and 2-nitronaphthalene are seemingly underestimated, while the remaining compounds might be overestimated. As mentioned earlier, a fraction of 9-fluorenone might originate from degradation of 9,10-phenanthrenequinone. However, the dominant presence of 9-fluorenone is supported by findings from previous research, as mentioned above. A further comparison with literature data on atmospheric concentrations of nitro- and oxy-PAHs is presented in Section 4.6.1.

Since many of the quantified analytes fell in the range below the lowest calibration standard, a more precise quantification could be carried out by analyzing more diluted calibration standards. This was not carried out due to a limited time frame of the project.

As seen in Table 4.5, the field blanks were free from all target compounds, except 9-fluorenone and 1-nitronaphthalene. These analytes were found to be the most abundant compounds in

gaseous phase, and it should be noted that contaminations during sampling, transport and storage can occur to a small extent.

4.6.1 Comparison with literature data from other sites

Table 4.4 presents a comparison of the atmospheric levels of nitro- and oxy-PAHs found in Longyearbyen with reported concentrations from other sites. Since this study took place in a remote area (after all, Longyearbyen is a small community) during winter and spring, the levels were compared with studies from rural sites, investigated during winter (except for Li et al. (2015), which reported annual means). However, it should be noted that the different studies investigated slightly different compounds of nitro- and oxy-PAHs, used different analytical methods and reported lower LOQs than in this study.

As can be seen in Table 4.4, the levels in Longyearbyen were far below the reported levels from rural areas in France, United Kingdom and China. This is probably due to smaller presence of emission sources in Longyearbyen, as the other sites were located outside larger cities, which bring along more pollution from power plants and traffic.

Table 4.4: Comparison of atmospheric levels of nitro- and oxy-PAHs in Longyearbyen with literature data from other sites. It should be noted that the different studies investigated slightly different compounds of nitro- and oxy-PAHs, used different analytical methods and reported different LOQs. In addition, note that some concentrations are given in pg m^{-3}, while others are given in ng m^{-3}.

	This study [a]	Albinet et al. (2008)	Alam et al. (2015)	Li et al. (2015)
Season	Winter/spring	Winter	Winter	Annual
Location	Longyearbyen, Svalbard	Chamonix valley, France	Birmingham, United Kingdom	Wuwei, China
Type of site	Urban/rural	Rural	Rural	Rural
Total oxy-PAHs	570.4 pg m^{-3}	5.8 ng m^{-3}	1.6 ng m^{-3}	27.5 ng m^{-3}
Total nitro-PAHs	64.2 pg m^{-3}	199.9 pg m^{-3}	1.7 ng m^{-3}	555.0 pg m^{-3}

[a] The reported concentrations are the maximum concentrations found in this study

Table 4.5: Overview of sample results (part 1). The results for the field blanks are given in ng, while the results for the samples are given in pg m^{-3}.

Compound	UFB		NFB		U1		U2		N1		N2	
	filter	PUF	filter	PUF	filter	PUF	filter	PUF	filter	PUF	filter	PUF
1,4-Naphthoquinone	n.d. [a]	n.d.	n.d.	n.d.	**25.4** [b c] **(0.9)**	n.d.	**34.9 (1.7)**	n.d.	*3.8* [d] *(0.4)*	n.d.	**33.3 (1.1)**	n.d.
1-Nitronaphthalene	*3.5 (0.0)*	n.d.	*3.7 (0.0)*	*3.7 (0.0)*	*17.8 (0.1)*	**30.4 (0.1)**	*14.0 (0.0)*	**26.3 (0.1)**	*14.2 (0.2)*	*13.5 (0.1)*	*13.9 (0.0)*	*14.0 (0.1)*
2-Nitronaphthalene	n.d.	n.d.	n.d.	n.d.	n.d.	*16.0 (0.1)*	n.d.	*15.7 (0.1)*	n.d.	n.d.	n.d.	*13.1 (0.0)*
9-Fluorenone	*3.2 (0.0)*	*2.8 (0.0)*	n.q. [e]	*4.1 (0.0)*	**59.6 (0.1)**	**25.2 (0.3)**	**120.0 (0.0)**	*11.8 (0.1)*	**40.3 (0.2)**	*13.6 (0.1)*	**251.6 (0.0)**	*13.9 (0.0)*
4-Nitrobiphenyl	n.d.	n.d.	n.d.	n.d.	n.d.	n.d.	n.d.	n.d.	n.d.	n.d.	n.d.	n.d.
9,10-Anthraquinone	n.d.	n.d.	n.d.	n.d.	n.d.	n.d.	**67.9 (9.2)**	n.d.	**19.9 (0.1)**	n.d.	**58.4 (1.1)**	n.d.
Benzo(a)fluoren-11-one	n.d.	n.d.	n.d.	n.d.	n.d.	n.d.	*40.9 (0.8)*	n.d.	n.d.	n.d.	**61.3 (0.3)**	n.d.
Benzanthrone	n.d.	n.d.	n.d.	n.d.	n.d.	n.d.	n.d.	n.d.	n.d.	n.d.	**107.5 (1.7)**	n.d.
1,2-Benz[*a*]anthraquinone	n.d.	n.d.	n.d.	n.d.	n.d.	n.d.	n.d.	n.d.	n.d.	n.d.	**44.5 (0.4)**	n.d.

[a] n.d. denotes not detected
[b] Mean value (standard deviation)
[c] Values in bold denotes that the value is within the linear range of the calibration curve
[d] Values in italics denotes that the value is outside the linear range of the calibration curve
[e] n.q. denotes not quantified. This was due to low response of the ISTD

Table 4.6: Overview of sample results (part 2). The results are given in pg m^{-3}.

Compound	N3		N4			N5		N6		
	filter	PUF	filter	U-PUF	L-PUF	filter	PUF	filter	U-PUF	L-PUF
1,4-Naphthoquinone	*13.5* [b d] *(0.0)*	n.d. [a]	n.d.	n.d.	n.d.	n.d.	n.d.	*3.3* *(0.0)*	n.d.	n.d.
1-Nitronaphthalene	*15.9* *(0.0)*	*18.0* *(0.0)*	*4.3* *(0.0)*	**11.7** [c] **(0.0)**	*4.3* *(0.0)*	*4.9* *(0.0)*	*6.3* *(0.0)*	*4.3* *(0.0)*	n.d.	n.d.
2-Nitronaphthalene	*15.0* *(0.0)*	*13.6*	n.d.	*5.9*	n.d.	n.d.	*6.6* *(0.0)*	n.d.	n.d.	n.d.
9-Fluorenone	**165.1** **(0.3)**	*13.9* *(0.3)*	**90.5** **(0.0)**	*3.9* *(0.0)*	*3.2* *(0.1)*	**159.5** **(1.2)**	**122.9** **(0.8)**	**36.9** **(0.2)**	**22.6** **(0.4)**	*3.1* *(0.0)*
4-Nitrobiphenyl	n.d.	n.d.	n.d.	n.d.	n.d.	n.d.	**8.1** **(0.2)**	n.d.	n.d.	n.d.
9,10-Anthraquinone	**48.0** **(0.4)**	n.d.	n.d.	n.d.	n.d.	n.d.	n.d.	**13.5** **(0.1)**	n.d.	n.d.
Benzo[*a*]fluoren-11-one	**49.1** **(0.2)**	n.d.	**18.6** **(0.1)**	n.d.	n.d.	**27.9** **(0.5)**	n.d.	*12.1* *(0.0)*	n.d.	n.d.
Benzanthrone	n.d.	n.d.	n.d.	n.d.	n.d.	n.d.	n.d.	n.d.	n.d.	n.d.
1,2-Benz[*a*]anthraquinone	**38.5** **(1.4)**	n.d.	**13.3** **(1.2)**	n.d.	n.d.	**18.6** **(1.3)**	n.d.	*11.1* *(0.0)*	n.d.	n.d.

[a] n.d. denotes not detected
[b] Mean value (standard deviation)
[c] values in bold denotes that the value is within the linear range of the calibration curve
[d] values in italics denotes that the value is outside the linear range of the calibration curve

Table 4.7: Overview of sample results (part 3). The results are given in pg m^{-3}.

Compound	N7		N8		N9			N10		
	filter	PUF	filter	PUF	filter	U-PUF	L-PUF	filter	U-PUF	L-PUF
1,4-Naphthoquinone	n.d. [a]	n.d.	**12.3** [b c] **(0.2)**	n.d.	*0.6* [d] *(0.0)*	n.d.	n.d.	n.d.	n.d.	n.d.
1-Nitronaphthalene	*4.6 (0.0)*	*6.8 (0.1)*	*5.5 (0.0)*	*6.3 (0.0)*	*2.1 (0.0)*	**7.3 (0.0)**	n.d.	*2.3 (0.0)*	**8.0 (0.0)**	n.d.
2-Nitronaphthalene	n.d.	*4.4 (0.0)*	*4.3 (0.0)*	n.d.	n.d.	**3.4 (0.0)**	n.d.	n.d.	**3.7 (0.0)**	n.d.
9-Fluorenone	**47.1 (0.8)**	**5.4 (0.1)**	**50.1 (0.3)**	*4.2 (0.0)*	**17.2 (0.1)**	**46.1 (0.2)**	**2.2 (0.1)**	**18.2 (0.1)**	**50.2 (0.7)**	*1.5 (0.0)*
4-Nitrobiphenyl	n.d.	n.d.	n.d.	n.d.	n.d.	n.d.	n.d.	n.d.	n.d.	n.d.
9,10-Anthraquinone	n.d.	n.d.	**12.4 (0.3)**	n.d.	**6.6 (0.0)**	n.d.	n.d.	**5.9 (0.9)**	n.d.	n.d.
Benzo(a)fluoren-11-one	n.d.	n.d.	*11.8 (0.2)*	n.d.	*4.5 (0.1)*	n.d.	n.d.	*4.6 (0.1)*	n.d.	n.d.
Benzanthrone	n.d.	n.d.	n.d.	n.d.	n.d.	n.d.	n.d.	n.d.	n.d.	n.d.
1,2-Benz[*a*]anthraquinone	n.d.	n.d.	*10.0 (0.0)*	n.d.	*4.1 (0.0)*	n.d.	n.d.	*4.4 (0.1)*	n.d.	n.d.

[a] n.d. denotes not detected
[b] Mean value (standard deviation)
[c] values in bold denotes that the value is within the linear range of the calibration curve
[d] values in italics denotes that the value is outside the linear range of the calibration curve

4.6.2 Distribution between particulate and gaseous phase

Figure 4.3 presents the total nitro- and oxy-PAH concentrations measured in each sample, showing the distribution in particulate and gaseous phase. In general, oxy-PAHs were predominant in particulate phase, while nitro-PAHs were either evenly distributed between the phases or more dominant in gaseous phase.

The nitro-PAHs detected in the air samples were mainly 1-nitronaphthalene and 2-nitronaphthalene, which are among the lightest nitro-PAHs, as they consist of two aromatic rings. Their dominant presence in gaseous phase corresponds to earlier research (Feilberg et al., 1999). 4-Nitrobiphenyl was detected in one PUF sample (N5), and is also a compound of two aromatic rings.

The quantified oxy-PAHs vary in molecular weight, where 1,4-naphthoquinone consists of two rings, 9,10-anthraquinone and 9-fluorenone consist of three rings and 1,2-benz[*a*]anthraquinone, benzanthrone and benzo[*a*]fluoren-11-one consist of four rings. The lighter compounds were expected to be dominant in gaseous phase. However, 9-fluorenone was the only oxy-PAH detected in PUF samples, but it should be noticed that this compound was mostly present in particulate phase as well. Albinet et al. (2008) reported that the fraction in particulate phase increased when the ambient air temperature was low, and this might explain the absence of oxy-PAHs in gaseous phase. The temperatures during sampling in this work were up to 25 °C lower than the temperatures for Albinet et al. (2008). On the other hand, this aspect was expected to apply for both nitro- and oxy-PAHs, which was not the case in this work.

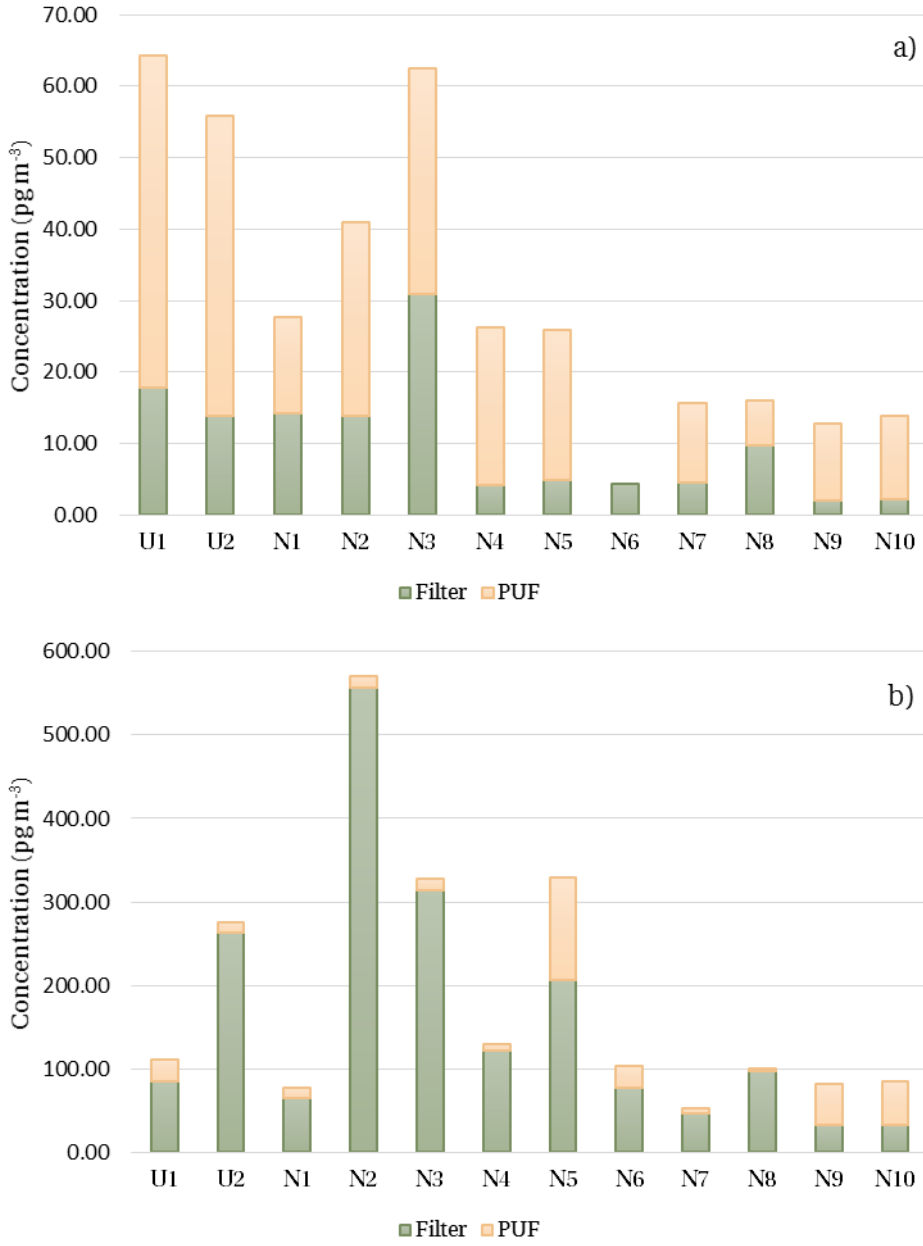

Figure 4.3: Total concentration of a) nitro-PAHs and b) oxy-PAHs in collected air samples.

4.6.3 Trends and correlations with weather conditions

Figure 4.4 presents how the concentrations of the individual nitro- and oxy-PAHs varied among the samples. 4-Nitrobiphenyl and benzanthrone were not included in the plots as they were present in only one sample each (N5 and N2, respectively). The levels of the individual compounds were highly correlated, following each other's trends, especially when looking at the group of nitro-PAHs and oxy-PAHs separately.

Considering weather conditions, a correlation was found between precipitation and levels of nitro- and oxy-PAHs. The highest levels were found in sample U2, N2, N3 and N5, all taken on days without precipitation. This is reasonable as particulate PAHs are likely to undergo wet deposition with precipitation (Kim et al., 2013).

The dominant wind direction in Longyearbyen is from south-east. Therefore, the original plan was to carry out the sampling program north-west of the coal power plant, as combustion processes are believed to be major emission sources of PAHs and derivatives. Due to logistical difficulties, the sampling campaign was moved to the old Aurora Station, south-west of the power plant. However, changes in wind direction were observed multiple times during the sampling campaign, which can be seen in the wind rose plots in Figure A.1 to A.11 in Appendix A.2.

As mentioned in Section 3.1, emissions from the power plant were expected to reach the old Aurora Station when the wind direction was from north-west. In addition, wind from north-west was expected to increase the levels of nitro- and oxy-PAHs at the roof of UNIS as well. As can be seen in the wind rose plots in Appendix A.2, there was wind dominating from north-west during sampling of U2, N2 and N8. There was also some wind from north during sampling of N9 and N10. The levels of nitro- and oxy-PAHs in sample N8, N9 and N10 were low, probably due to precipitation, as mentioned above. However, three of the oxy-PAHs were most abundant in sample U2 and N2, which may indicate that their major emission source is the coal power plant. At the other hand, sample N3 and N5 had levels of oxy-PAHs close to the levels in U2 and N2, even though the wind was from south-east during these samples. This may indicate that traffic might be a major emission source as well. Nevertheless, a more extensive sampling campaign is a necessity in order to assess the emission sources.

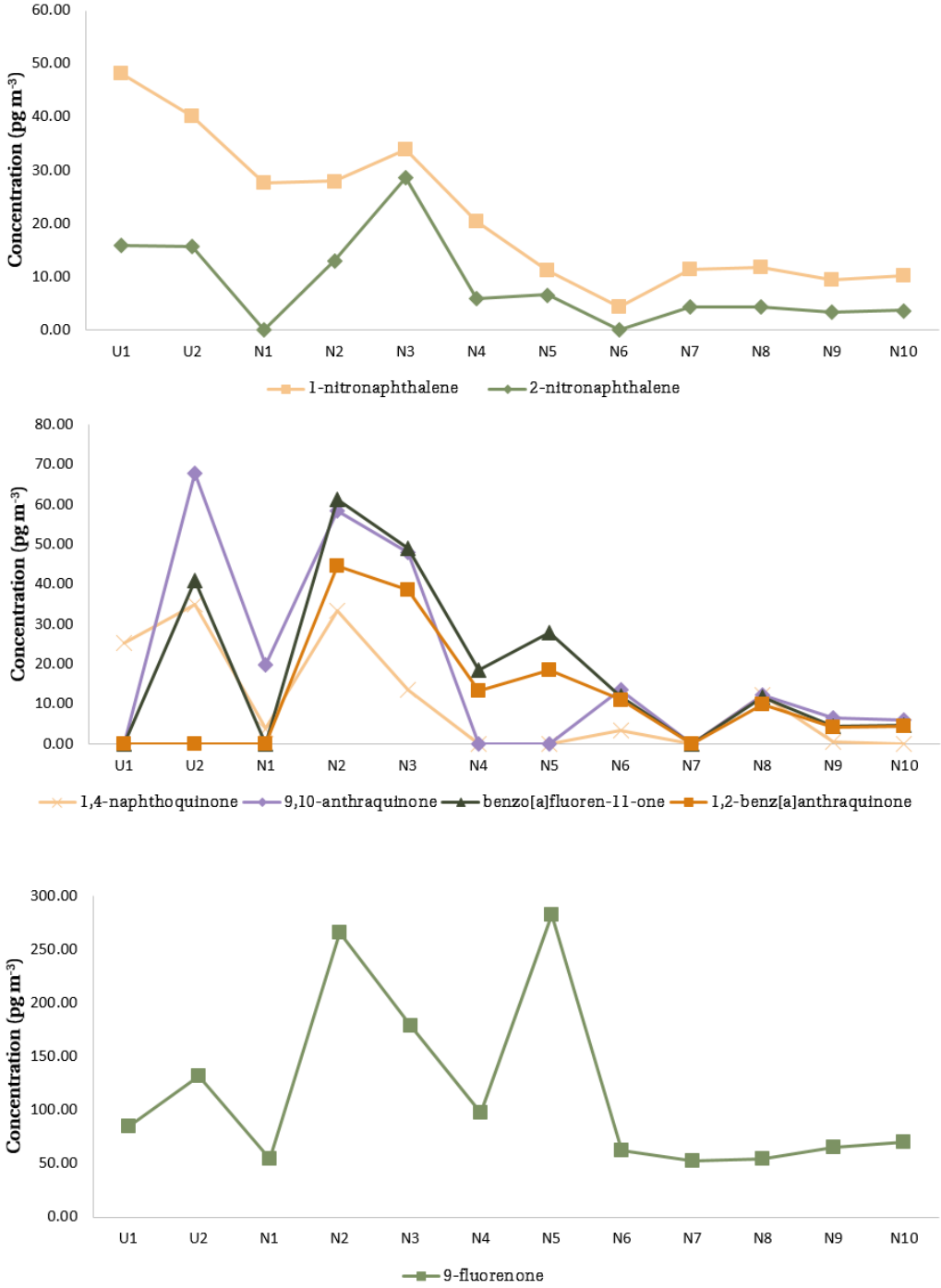

Figure 4.4: Concentrations of individual nitro- and oxy-PAHs in the collected air samples (gaseous and particulate phase).

Since atmospheric degradation is dependent on the amount of sunlight, a trend was expected to be found throughout the sampling period, as the period of daylight increase rapidly for each day during the Arctic spring. However, there was precipitation during the sampling of the five last samples, and it is therefore uncertain if the decrease in nitro- and oxy-PAHs can be attributed to longer days or more precipitation.

4.6.4 Repeatability

As seen in Table 4.5, 4.6 and 4.7, the instrumental precision was acceptable, as the standard deviations were reasonably low.

Repeatability of the method was investigated by looking at the results from two parallel samples taken at the old Aurora Station (sample N9 and sample N10). As can be seen in Table 4.7 and in Figure 4.3 and 4.4, the results from sample N9 and N10 are almost identical, in both filter and PUF samples. This indicates that the whole method, including sampling, storage, sample preparation and analysis, is of high repeatability, although more parallel samples are necessary in order to verify the repeatability.

4.6.5 Breaktrough

The most abundant compounds, 9-fluorenone and 1-nitronaphthalene, were also the only compounds that were observed in events of breakthrough. Out of four samples, breakthrough was observed in one sample for 1-nitronaphthalene and in four samples for 9-fluorenone, and the measures of breakthrough are presented in Table 4.8. As mentioned in Section 2.2, the breakthrough effect is acceptable when B is less than 20%, but noteworthy when B approaches 50%. Therefore, breakthrough was negligible for sample N6, N9 and N10, but remarkable for sample N4. Sample N4 had a higher concentration of 1-nitronaphthalene than sample N6, N9 and N10, which might be the reason for higher value of breakthrough. However, there is no obvious reason why high value of breakthrough was observed for 9-fluorenone in this sample, as the concentration of gaseous phase 9-fluorenone was less in sample N4 than in the other samples.

Table 4.8: Measures of breakthrough (B) for the analytes where this event was observed, given in %.

Sample	9-Fluorenone	1-Nitronaphthalene
N4	45	27
N6	12	-[a]
N9	4	-
N10	3	-

[a] - donotes breakthrough not observed.

4.6.6 Environmental concern

The presence of nitro- and oxy-PAHs in ambient air in Longyearbyen indicates that these pollutants may also be present in other environmental matrices. As mentioned in Section 2.1.3, atmospheric nitro- and oxy-PAHs can deposit and adsorb onto soil and sediments. In addition, oxy-PAHs have the potential to spread via surface water and ground water as they are more polar than PAHs and other derivatives. Research on the environmental consequences of nitro- and oxy-PAHs is sparse, but their mutagenic properties makes them a concern as they can enter arctic ecosystems. However, as mentioned in Section 4.6.1, the levels in Longyearbyen were far below concentrations reported in literature from other sites of the world.

5 Conclusion

The analytical method tested in this study made it possible to identify 27 out of 32 nitro- and oxy-PAHs in gaseous and particulate phase of air samples. Quantification could be carried out for 19 compounds. The QuEChERS extraction method was shown to be suitable for sample extraction and clean-up, although some samples had low recoveries of the internal standards that might result in inaccurate quantification. High band broadening during the GC/NICI-MS analyses resulted in low sensitivity of compounds of high molecular weight, which led to unsuccessful identification and quantification of many target compounds. However, the analytes of lower molecular weight could be quantified with acceptable LOD, LOQ, linearity, precision and accuracy.

Nine of the target compounds were detected and quantified in samples from Longyearbyen. The majority of the analytes were present in particulate phase, except 1- and 2-nitronaphthalene that were mainly present in gaseous phase. The total levels of nitro- and oxy-PAHs varied from 68.3 to 611.4 pg m^{-3}, where 9-fluorenone was the most abundant compound. Levels decreased at days with precipitation, which may be due to wet deposition. Highest levels were reported at days with wind from north-west, which could indicate that the coal power plant is the major emission source of nitro- and oxy-PAHs in Longyearbyen. However, vehicle emissions are also believed to be a significant emission source, as nitro- and oxy-PAHs were detected at days with wind from south-east as well. The concentrations of nitro- and oxy-PAHs in Longyearbyen were far below reported concentrations of these compounds in other areas of the world, but their presence may still be a concern for arctic ecosystems due to their potential toxic effects.

6 Suggestions for further work

Future research should aim at optimizing the GC/NICI-MS conditions in order to identify and quantify all target compounds. Less band broadening and less asymmetry is essential for quantification of late eluting compounds at trace levels. Different oven temperature programs, injection temperatures and flow rates might be useful aspects to investigate in the method optimization. In order to determine levels of 1-indanone, the reason for contaminated blanks has to be assessed. Future research should also use calibration standards of lower concentrations than 25 pg μL^{-1}, in order to extend the calibration curve in the lower range.

It would be interesting to carry out more extensive sampling programs in Longyearbyen. The most dominant wind direction in Longyearbyen is from south-east, and a sampling site north-west of the coal power plant would be ideal to assess the contribution to atmospheric nitro- and oxy-PAHs from emissions of coal combutions. In addition, a more extensive sampling program is necessary in order to assess how the amount of sunlight affects the levels of nitro- and oxy-PAHs in air. Several sampling sites along a suitable transect from the power plant would be optimal for monitoring of degradation products of PAHs released from the power plant. However, the logistics are challenging, as the sites have to be easily accessible and must have electricity supply for the high volume air samplers.

References

Alam, M. S., Keyte, I. J., Yin, J., Stark, C., Jones, A. M., and Harrison, R. M. (2015). Diurnal variability of polycyclic aromatic compound (PAC) concentrations: Relationship with meteorological conditions and inferred sources. *Atmospheric Environment*, 122:427–438.

Albinet, A., Leoz-Garziandia, E., Budzinski, H., and Villenave, E. (2006). Simultaneous analysis of oxygenated and nitrated polycyclic aromatic hydrocarbons on standard reference material 1649a (urban dust) and on natural ambient air samples by gas chromatography-mass spectrometry with negative ion chemical ionisation. *Journal of Chromatography A*, 1121(1):106–113.

Albinet, A., Leoz-Garziandia, E., Budzinski, H., and Villenave, E. (2007). Polycyclic aromatic hydrocarbons (PAHs), nitrated PAHs and oxygenated PAHs in ambient air of the Marseilles area (South of France): Concentrations and sources. *Science of the Total Environment*, 384(1-3):280–292.

Albinet, A., Leoz-Garziandia, E., Budzinski, H., Villenave, E., and Jaffrezo, J. L. (2008). Nitrated and oxygenated derivatives of polycyclic aromatic hydrocarbons in the ambient air of two French alpine valleys. Part 1: Concentrations, sources and gas/particle partitioning. *Atmospheric Environment*, 42(1):43–54.

Albinet, A., Nalin, F., Tomaz, S., Beaumont, J., and Lestremau, F. (2014). A simple QuEChERS-like extraction approach for molecular chemical characterization of organic aerosols: Application to nitrated and oxygenated PAH derivatives (NPAH and OPAH) quantified by GC-NICIMS. *Analytical and Bioanalytical Chemistry*, 406(13):3131–3148.

Arey, J. (1986). Reactions of Fluoranthene and Pyrene With the OH Radical in the Presence of NOx. *Atmospheric Environment*, 20(12):2339–2345.

Arey, J. (1998). Atmospheric Reactions of PAHs Including Formation of Nitroarenes. In Neilson, A. H., editor, *PAHs and Related Compounds: Chemistry*, pages 347–385. Springer Berlin Heidelberg, Berlin, Heidelberg.

Atkinson, R., Arey, J., Zielinska, B., and Aschmann, S. M. (1990). Kinetics and Nitro-Products of the Gas-Phase OH and NO3 Radical-Initiated Reactions of Naphthalene-d8, Fluoranthene-d10, and Pyrene. *International Journal of Chemical Kinetics*, 22(9):999–1014.

Bayona, J. M., Casellas, M., Fernandez, P., Solanas, A. M., and Albaiges, J. (1994). Sources and Seasonal Variability of Mutagenic-Agents in the Barcelona City Aerosol. *Chemosphere*, 29(3):441–450.

Boström, C. E., Gerde, P., Hanberg, A., Jernstrom, B., Johansson, C., Kyrklund, T., Rannug, A., Tornqvist, M., Victorin, K., and Westerholm, R. (2002). Cancer risk assessment, indicators, and guidelines for polycyclic aromatic hydrocarbons in the ambient air. *Environmental Health Perspective*, 110(3):451–488.

Casellas, M., Fernández, P., Bayona, J., and Solanast, A. (1995). Bioassay-directed chemical analysis of genotoxic components in urban airborne particulate matter from Barcelona (Spain). *Chemosphere*, 30(4):725–740.

Castells, P., Santos, F. J., and Galceran, M. T. (2003). Development of a sequential supercritical fluid extraction method for the analysis of nitrated and oxygenated derivatives of polycyclic aromatic hydrocarbons in urban aerosols. *Journal of Chromatography A*, 1010(2):141–151.

Cochran, R. E., Dongari, N., Jeong, H., Beránek, J., Haddadi, S., Shipp, J., and Kubátová, A. (2012). Determination of polycyclic aromatic hydrocarbons and their oxy-, nitro-, and hydroxy-oxidation products. *Analytica Chimica Acta*, 740:93–103.

Delhomme, O., Millet, M., and Herckes, P. (2008). Determination of oxygenated polycyclic aromatic hydrocarbons in atmospheric aerosol samples by liquid chromatography-tandem mass spectrometry. *Talanta*, 74(4):703–710.

Di Filippo, P., Pomata, D., Riccardi, C., Buiarelli, F., and Gallo, V. (2015). Oxygenated polycyclic aromatic hydrocarbons in size-segregated urban aerosol. *Journal of Aerosol Science*, 87:126–134.

Durant, J. L., Busby JR, W. F., Lafleur, A. L., Penman, B. W., and Crespi, C. L. (1996). Human cell mutagenicity of oxygenated, nitraed and unsubstitued polycyclic aromatic hydrocarbons associated with urban aerosols. *Mutation Research - Genetic Toxicology*, 371:123–157.

Feilberg, A., Kamens, R. M., Strommen, M. R., and Nielsen, T. (1999). Modeling the formation, decay, and partitioning of semivolatile nitro-polycyclic aromatic hydrocarbons (nitronaphthalenes) in the atmosphere. *Atmospheric Environment*, 33(8):1231–1243.

Feilberg, A. and Nielsen, T. (2000). Effect of aerosol chemical composition on the photodegradation of nitro-polycyclic aromatic hydrocarbons. *Environmental Science & Technology*, 34(5):789–797.

Garstad, J. B. (2016). *Utvikling av en gasskromatografi/massespektrometrimetode for kvantifisering av nitro- og oksy-polysykliske aromatiske hydrokarboner (N-/O-PAH) i jordprøver*. Master's thesis. Norwegian University of Life Sciences.

Godula, M., Hajšlová, J., Maštouska, K., and Křivánková, J. (2001). Optimization and application of the PTV injector for the analysis of pesticide residues. *Journal of Separation Science*, 24(5):355–366.

Greenberg, A., Lwo, J.-H., Altherholt, T. B., Rosen, R., Hartman, T., Butler, J., and Louis, J. (1993). Bioassay-directed fractionation of organic compounds associated with airborne particulate matter: an interseasonal study. *Atmospheric Environment*, 27A(10):1609–1626.

Gross, J. H. (2004). *Mass Spectrometry: A Textbook*. Springer Science & Business Media.

Harris, D. C. (2010). *Quantitative Chemical Analysis*. Freeman, 8th edition.

Hart, K. M., Isabelle, L. M., and Pankow, J. F. (1992). High-Volume Air Sampler for Particle and Gas Sampling. 1. Design and Gas Sampling Performance. *Environmental Science and Technology*, 26(5):1048–1052.

Harvey, D. (2000). *Modern Analytical Chemistry*. McGraw-Hill, New York.

Hayakawa, K., Nakamura, A., Terai, N., Kizu, R., and Ando, K. (1997). Nitroarene concentrations and direct-acting mutagenicity of diesel exhaust particulates fractionated by silica-gel column chromatography. *Chemical & Pharmaceutical Bulletin*, 45(11):1820–1822.

Hubert, P., Chiap, P., Crommen, J., Boulanger, B., Chapuzet, E., Mercier, N., Bervoas-Martin, S., Chevalier, P., Grandjean, D., Lagorce, P., Lallier, M., Laparra, M. C., Laurentie, M., and Nivet, J. C. (1999). The SFSTP guide on the validation of chromatographic methods for drug bioanalysis: From the Washington Conference to the laboratory. *Analytica Chimica Acta*, 391(2):135–148.

Hung, H., Blanchard, P., Halsall, C., Bidleman, T., Stern, G., Fellin, P., Muir, D., Barrie, L., Jantunen, L., Helm, P., Ma, J., and Konoplev, A. (2005). Temporal and spatial variabilities of

atmospheric polychlorinated biphenyls (PCBs), organochlorine (OC) pesticides and polycyclic aromatic hydrocarbons (PAHs) in the Canadian Arctic: Results from a decade of monitoring. *Science of The Total Environment*, 342(1-3):119–144.

IARC (1989). Diesel and Gasoline Engine Exhaust and Some Nitroarenes. *IARC Monographs on the Evaluation of Carcinogenic Risks to Humans*, 46.

Keith, L. and Telliard, W. (1979). Priority pollutants: I-a perspective view. *Environmental Science & Technology*, 13(4):416–423.

Kelly, K. and Parnell, K. (2017). Technical Tips: How to Improve Late Eluting Peaks. Retrieved from https://www.phenomenex.com/Info/Page/gclateeluting (26/06/17).

Kielhorn, J., Wahnschaffe, U., and Mangelsdorf, I. (2004). Environmental Health Criteria 229: Selected nitro- and nitro-oxy-polycyclic aromatic hydrocarbons. *World Health Organization*.

Kim, K.-H., Jahan, S. A., Kabir, E., and Brown, R. J. (2013). A review of airborne polycyclic aromatic hydrocarbons (PAHs) and their human health effects. *Environment International*, 60:71–80.

Li, W., Wang, C., Shen, H., Su, S., Shen, G., Huang, Y., Zhang, Y., Chen, Y., Chen, H., Lin, N., Zhuo, S., Zhong, Q., Wang, X., Liu, J., Li, B., Liu, W., and Tao, S. (2015). Concentrations and origins of nitro-polycyclic aromatic hydrocarbons and oxy-polycyclic aromatic hydrocarbons in ambient air in urban and rural areas in northern China. *Environmental Pollution*, 197(x):156–164.

Liu, Y., Sklorz, M., Schnelle-Kreis, J., Orasche, J., Ferge, T., Kettrup, A., and Zimmermann, R. (2006). Oxidant denuder sampling for analysis of polycyclic aromatic hydrocarbons and their oxygenated derivates in ambient aerosol: Evaluation of sampling artefact. *Chemosphere*, 62(11):1889–1898.

Longyearbyen Lokalstyre (2012). Energiverket: Produksjon. Retrieved from www.lokalstyre.no (20/06/17).

Lundanes, Elsa, R. L. G. T. (2014). *Chromatography: Basic Principles, Sample Preparations and Related Methods*. John Wiley & Sons.

Lundstedt, S., White, P. A., Lemieux, C. L., Lynes, K. D., Lambert, I. B., and Oberg, L. (2007). Sources, Fate, and Toxic Hazards of Oxygenated Polycyclic Aromatic Hydrocarbons (PAHs) at PAH-contaminated Sites. *A Journal of the Human Environment*, 36(6):475–485.

MA, M. (2010). Wind rose of direction and intensity. MATLAB Central File Exchange. Retrieved from https://se.mathworks.com/matlabcentral/fileexchange/17748-wind-rose (22/06/17).

Macherey-Nagel (n.d.). SPE CHROMABOND Vacuum Manifolds: User Manual. Technical report.

Mallakin, A., George Dixon, D., and Greenberg, B. M. (2000). Pathway of anthracene modification under simulated solar radiation. *Chemosphere*, 40(12):1435–1441.

Meyer, S., Cartellieri, S., and Steinhart, H. (1999). Simultaneous determination of PAHs, hetero-PAHs (N, S, O), and their degradation products in creosote-contaminated soils. Method development, validation, and application to hazardous waste sites. *Analytical Chemistry*, 71(18):4023–4029.

Mitra, S. and Brukh, R. (2003). *Sample Preparation Techniques in Analytical Chemistry (Vol. 162)*. John Wiley & Sons, Hoboken, NJ.

Niederer, M. (1998). Determination of polycyclic aromatic hydrocarbons and substitutes (nitro-, Oxy-PAHs) in urban soil and airborne particulate by GC-MS and NCI-MS/MS. *Environmental science and pollution research international*, 5(4):209–216.

Nielsen, T. (1984). Reactivity of polycyclic aromatic hydrocarbons towards nitrating species. *Environmental Science & Technology*, 18(3):157–163.

Norwegian Meteorological Institute and NRK. Weather forecast from Yr. Retrieved from www.yr.no. (30/03/17).

Norwegian Polar Institute (2017). TopoSvalbard. Retrieved from toposvalbard.npolar.no (26/06/17).

Oehme, M. (2007). *Quality control in organic trace analysis*. Applied Analytical Chemistry, Arlesheim and University of Basel, Basel.

Pohanish, R. P. (2008). *Sittig's handbook of toxic and hazardous chemicals and carcinogens*. William Andrew.

Poole, C. F. (2003). *The Essence of Chromatography*. Elsevier, Detroit, MI, 1st edition.

Reisen, F. and Arey, J. (2005). Atmospheric Reactions Influence Seasonal PAH and Nitro-PAH Concentrations in the Los Angeles Basin. *Environmental Science & Technology*, 39(1):64–73.

Restek Corporation (2013). GC Troubleshooting tips. *Lit. Cat.# GNWC1723-UNV*.

Sasaki, J., Arey, J., and Harger, W. P. (1995). Formation of Mutagens from the Photooxidations of 2–4 ring PAH. *Environmental Science & Technology*, 29(5):1324–1335.

Sasaki, T. and Makino, Y. (2006). Effective injection in pulsed splitless mode for impurity profiling of methamphetamine crystal by GC or GC/MS. *Forensic Science International*, 160(1):1–10.

Sklorz, M., Briedé, J.-J., Schnelle-Kreis, J., Liu, Y., Cyrys, J., de Kok, T. M., and Zimmermann, R. (2007). Concentration of Oxygenated Polycyclic Aromatic Hydrocarbons and Oxygen Free Radical Formation from Urban Particulate Matter. *Journal of Toxicology and Environmental Health, Part A*, 70(21):1866–1869.

Tisch Environmental Inc. (n.d.). OPERATIONS MANUAL. TE-PUF Poly-Urethane Foam High Volume Sampler. Technical report, Tisch Environmental, Inc., Village of Cleves, Ohio.

UNIS. Aventdalen weather station. Retrieved from http://158.39.149.183/Adventdalen/index.html (30/03/17).

University of Pittsburgh (n.d). Mass Spectrometry Introduction. Retrieved from http://www.chem.pitt.edu/facilities/mass-spectrometry/mass-spectrometry-introduction (15/06/17).

Watson, A., Kennedy, D., and Bates, R. (1988). *Air pollution, the automobile, and public health*. National Academy Press, Washington, D.C.

Weschler, C. J. and Nazaroff, W. W. (2008). Semivolatile organic compounds in indoor environments. *Atmospheric Environment*, 42(40):9018–9040.

West, D. A., West, D. M., Holler, F. J., and Crouch, S. R. (2014). *Skoog and West's Fundamentals of Analytical Chemistry*. Brooks Cole, Cencage Learning, 9th edition.

Yu, D. S., Berlin, J. A., Penning, T. M., and Field, J. (2002). Reactive oxygen species generated by PAH o-quinones cause change-in-function mutations in p53. *Chemical Research in Toxicology*, 15(6):832–842.

Zhang, Y., Yang, B., Gan, J., Liu, C., Shu, X., and Shu, J. (2011). Nitration of particle-associated PAHs and their derivatives (nitro-, oxy-, and hydroxy-PAHs) with NO3 radicals. *Atmospheric Environment*, 45(15):2515–2521.

Zhuo, S., Du, W., Shen, G., Li, B., Liu, J., Cheng, H., Xing, B., and Tao, S. (2017). Estimating relative contributions of primary and secondary sources of ambient nitrated and oxygenated polycyclic aromatic hydrocarbons. *Atmospheric Environment*, 159:126–134.

Zielinska, B., Sagebiel, J., McDonald, J. D., Whitney, K., and Lawson, D. R. (2004). Emission Rates and Comparative Chemical Composition from Selected In-Use Diesel and Gasoline-Fueled Vehicles. *Journal of the Air & Waste Management Association*, 54(9):1138–1150.

A Additional sampling information

Weather data was retrieved from Adventdalen weather station, delivered by UNIS (temperature, wind speed and wind direction) and from Yr, delivered by Norwegian Meteorological Institute and NRK (precipitation).

A.1 Date, duration and weather conditions

Table A.1: Date, duration, ambient temperature, dominating wind direction and amount of precipitation for every sample.

Sample ID[a]	Start and stop time [dd/mm/yy h:min]	Duration [h]	Avg. T [°C]	Dom. wind direction[b]	Precipitation [mm]
U1	12/02/17 17:01 13/02/17 17:43	24.7	-5.9	SSE	0.0
U2	13/02/17 17:59 14/02/17 18:24	24.4	-11.4	NW	0.0
N1	16/02/17 11:55 17/02/17 11:11	23.3	-17.5	SE	0.2
N2	22/02/17 16:45 23/02/17 16:22	23.6	-11.9	NNW	0.0
N3	24/02/17 16:02 25/02/17 15:31	23.5	-20.3	ESE	0.0
N4	28/02/17 14:58 02/03/17 15:39	48.7	-16.7	ESE	0.0
N5	02/03/17 16:17 04/03/17 17:50	49.6	-11.4	SE	0.0
N6	04/03/17 18:22 06/03/17 16:49	46.5	-8.1	ESE	0.7
N7	08/03/17 15:29 10/03/17 15:06	47.6	-10.7	SE	1.0
N8	10/03/17 15:42 12/03/17 14:36	46.9	-19.3	NW	1.9
N9 & N10	12/03/17 15:15 17/03/17 16:31	121.1	-8.0	N and SE	3.6

[a] The first letter in the sample ID represents the sampling site. U = UNIS roof, N = The Old Aurora station
[b] N = North, E = East, S = South, W = West

A.2 Wind rose plots

Wind rose plots were created with MATLAB R2016b, using a wind rose function downloaded from MATLAB Central File Exchange (MA, 2010).

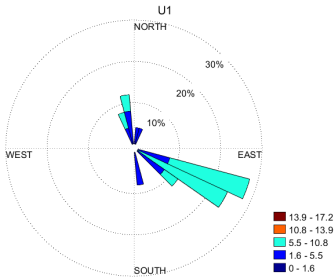

Figure A.1: Wind rose plot for sample U1.

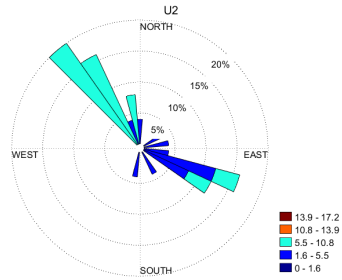

Figure A.2: Wind rose plot for sample U2.

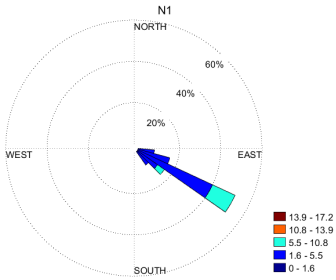

Figure A.3: Wind rose plot for sample N1.

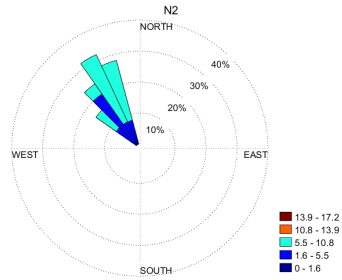

Figure A.4: Wind rose plot for sample N2.

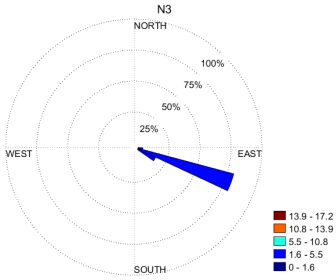

Figure A.5: Wind rose plot for sample N3.

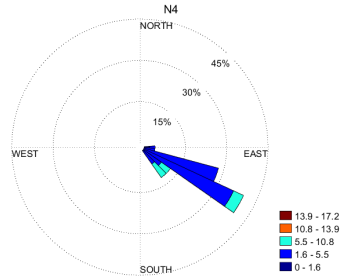

Figure A.6: Wind rose plot for sample N4.

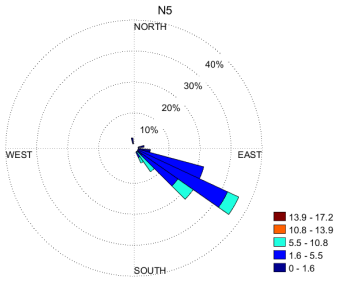

Figure A.7: Wind rose plot for sample N5.

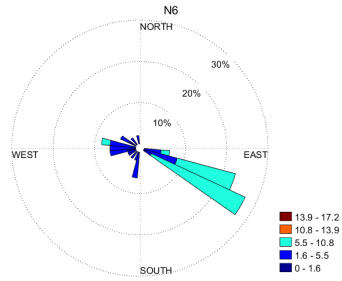

Figure A.8: Wind rose plot for sample N6.

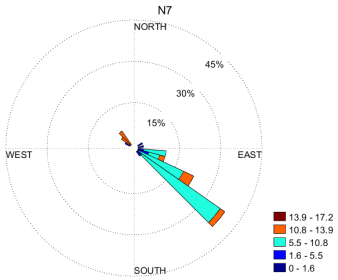

Figure A.9: Wind rose plot for sample N7.

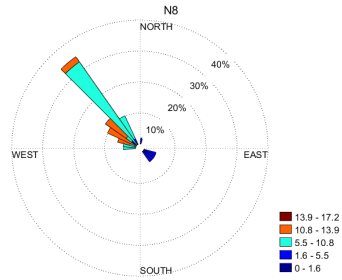

Figure A.10: Wind rose plot for sample N8.

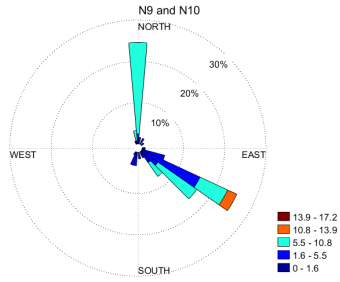

Figure A.11: Wind rose plot for sample N9 and N10.

A.3 Calibration of air samplers

AIR SAMPLER 5127 CALIBRATION

Time and date:	08.02.2017	16:00
Location:	UNIS roof	

CALIBRATION DATA

Magnehelic readings [inch H2O]	Slack tube left [inch H2O]	Slack tube right [inch H2O]	Slack tube sum [inch H2O]	Flow, slack (Qstd) [m3/min]	Flow, mag (corr) [m3/min]
90	4.8	4.9	9.7	0.320184109	9.932530865
80	4.5	4.5	9.0	0.308574588	9.364479906
70	4.0	4.1	8.1	0.292962681	8.759668853
60	3.6	3.6	7.2	0.27645653	8.109877491
50	3.1	3.2	6.3	0.258882221	7.403271401
40	2.6	2.7	5.3	0.237808728	6.621687244
30	2.1	2.1	4.2	0.212174316	5.734549369
20	1.6	1.6	3.2	0.185753678	4.682239953
12	1.0	1.0	2.0	0.147761775	3.626847472

Ambient pressure	772.563408	[mmHg]
Ambient temperature	276.35	[K]
Calibration slope m	10.32435	[-]
Calibration intercept b	-0.04489	[-]

CALIBRATION RESULTS

R^2	0.996798459	[-]
Significance	5.41041E-10	[-]
Sampler slope m	36.87301083	[-]
Sampler intercept b	-0.219837234	[-]

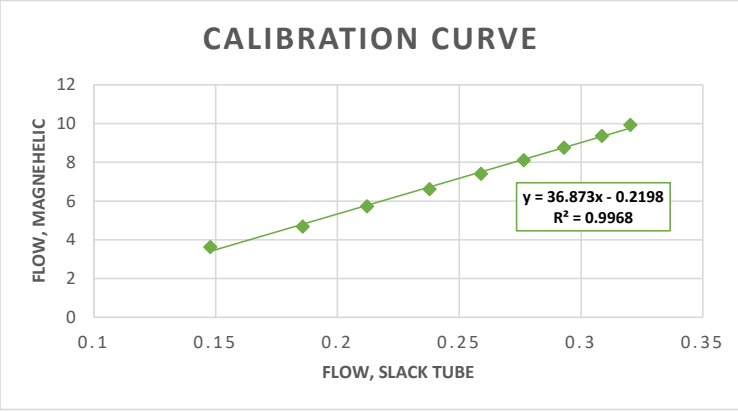

AIR SAMPLER 5127 CALIBRATION

Time and date: 14.03.2017 12:30

Location: Old aurora station

CALIBRATION DATA

Magnehelic readings [inch H2O]	Slack tube left [inch H2O]	Slack tube right [inch H2O]	Slack tube sum [inch H2O]	Flow, slack (Qstd) [m3/min]	Flow, mag (corr) [m3/min]
90	5.0	4.8	9.8	0.315948354	9.749198555
80	4.6	4.4	9.0	0.302959245	9.191632546
70	4.2	3.7	7.9	0.284116263	8.597984953
60	3.8	3.2	7.0	0.267698361	7.960187287
50	3.4	2.6	6.0	0.248163056	7.266623565
40	3.0	2.0	5.0	0.226919674	6.499465704
30	2.5	1.4	3.9	0.200917977	5.62870241
20	2.1	0.9	3.0	0.176751271	4.595816273
10	1.5	0.1	1.6	0.13025354	3.249732852

Ambient pressure	733.999579	[mmHg]
Ambient temperature	272.523	[K]
Calibration slope m	10.32435	[-]
Calibration intercept b	-0.04489	[-]

CALIBRATION RESULTS

R^2	0.998572595	[-]
Significance	3.19955E-11	[-]
Sampler slope m	35.35921384	[-]
Sampler intercept b	-1.490530624	[-]

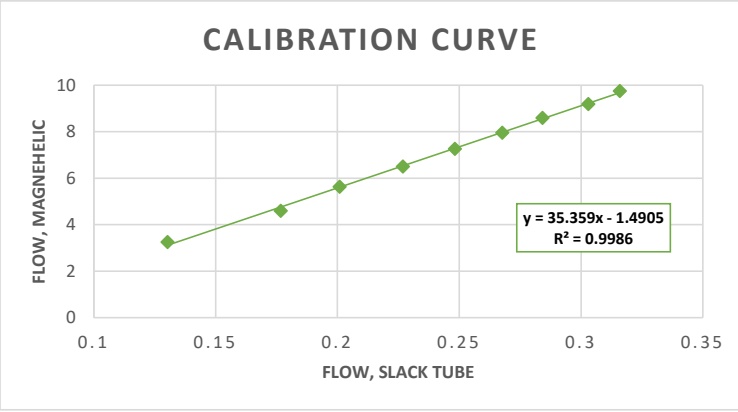

AIR SAMPLER 5128 CALIBRATION

Time and date: 14.03.2017 12:30

Location: Old aurora station

CALIBRATION DATA

Magnehelic readings [inch H2O]	Slack tube left [inch H2O]	Slack tube right [inch H2O]	Slack tube sum [inch H2O]	Flow, slack (Qstd) [m3/min]	Flow, mag (corr) [m3/min]
90	4.7	4.9	9.6	0.312752368	9.749198555
80	4.3	4.4	8.7	0.297940211	9.191632546
70	3.9	4.0	7.9	0.284116263	8.597984953
60	3.3	3.4	6.7	0.261993344	7.960187287
50	2.8	2.9	5.7	0.24198952	7.266623565
40	2.3	2.4	4.7	0.220139243	6.499465704
30	1.7	1.8	3.5	0.190564818	5.62870241
20	1.1	1.2	2.3	0.155303445	4.595816273
14	0.9	1.0	1.9	0.141550384	3.845135765

Ambient pressure	733.999579	[mmHg]
Ambient temperature	272.523	[K]
Calibration slope m	10.32435	[-]
Calibration intercept b	-0.04489	[-]

CALIBRATION RESULTS

R^2	0.997810733	[-]
Significance	1.43004E-10	[-]
Sampler slope m	33.25067344	[-]
Sampler intercept b	-0.744755059	[-]

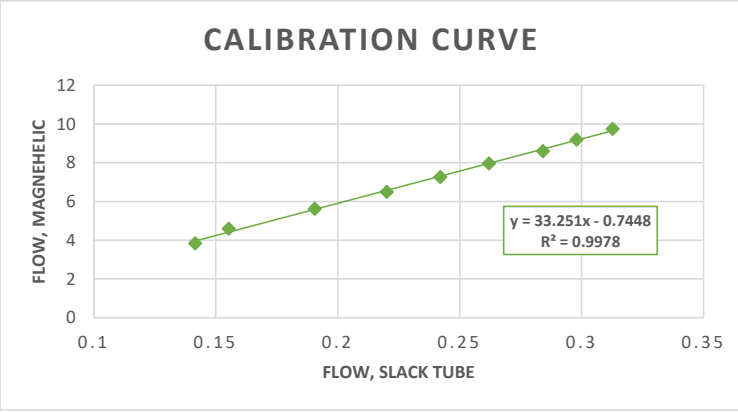

B Standards, chemicals and materials

B.1 Standards

Table B.1: List of standards used for identification and quantification. All standards were purchased from CHIRON AS, Trondheim, Norway.

Name	Concentration [ng/µL]	Solvent	CAS no.
9,10-Anthraquinone	1000	toluene	84-65-1
Benzanthrone	1000	toluene	82-05-3
1,2-Benzo[*a*]anthraquinone	1000	toluene	2498-66-0
Benzo[*a*]fluoren-11-one	200	toluene	479-79-8
6H-Benzo[*c,d*]pyren-6-one	200	toluene	3074-00-8
4H-Cyclopenta[*d,e,f*]phenanthren-4-one	1000	toluene	5737-13-3
9-Fluorenone	1000	isooctane	486-25-9
1-Indanone	1000	toluene	83-33-0
2-Methyl-9,10-anthraquinone	1000	isooctane	84-54-8
1,4-Naphthoquinone	1000	isooctane	130-15-4
9,10-Phenanthrenequinone	1000	toluene	84-11-7
9-Fluorenone-d_8	1000	toluene	137219-34-2
2,7-Dinitrofluorene	100	toluene	5405-53-8
1,3-Dinitropyrene	100	toluene	75321-20-9
1,6-Dinitropyrene	100	toluene	42397-64-8
1,8-Dinitropyrene	100	toluene	42397-65-9
5-Nitroacenaphthene	1000	toluene	602-87-9
2-Nitroanthracene	200	toluene	3586-69-4
9-Nitroanthracene	100	toluene	602-60-8
7-Nitrobenz[*a*]anthracene	100	toluene	20268-51-3
6-Nitrobenzo[*a*]pyrene	100	toluene	63041-90-7
4-Nitrobiphenyl	100	toluene	92-93-3
6-Nitrochrysene	100	toluene	7496-02-8
2-Nitrofluoranthene	100	toluene	13177-29-2
3-Nitrofluoranthene	100	toluene	892-21-7
2-Nitrofluorene	100	toluene	607-57-8
1-Nitronaphthalene	100	toluene	86-57-7
2-Nitronaphthalene	100	toluene	581-89-5
9-Nitrophenanthrene	1000	isooctane	954-46-1
1-Nitropyrene	100	toluene	5522-43-0
2-Nitropyrene	100	toluene	789-07-1
4-Nitropyrene	100	toluene	57835-92-4
9-Methylcarbazole	1000	toluene	1484-12-4
2-Nitrobiphenyl-d_9	1000	toluene	38537-53-0
Fluoranthene-d_{10}		solid	93951-69-0

B.2 Chemicals

UNIS

Acetone, Ph.Eur grade, VWR International, Oslo, Norway

Acetonitrile, for gas chromatography ECD and FID, Merck KGaA, Darmstadt, Germany

Dichloromethane, for gas chromatography, Merck KGaA, Darmstadt, Germany

Cyclohexane, for gas chromatography, Merck KGaA, Darmstadt, Germany

Methanol, for gas chromatography EDC and FID, Merck KGaA, Darmstadt, Germany

n-Pentane, for GC - capillary grade, VWR International, Oslo, Norway

CHROMABOND SiOH neutral, 3 mL, 500 mg, Macherey Nagel, Düren, Germany

Nitrogen, 5.0, AGA AS, Porsgrunn, Norway

N-PAH and O-PAH standards (see Table B.1), CHIRON AS, Trondheim, Norway

NMBU

Acetone, Ph.Eur grade, Merck KGaA, Darmstadt, Germany

Cyclohexane, for HPLC, VWR International, Oslo, Norway

n-Hexane, SupraSolv grade, Merck KGaA, Darmstadt, Germany

Toluene, for pesticide residue analysis, Fluka Analytical, Sigma-Aldrich, Oslo, Norway

Helium, 6.0, AGA AS, Porsgrunn, Norway Nitrogen, 6.0, AGA AS, Porsgrunn, Norway

Methane, 6.0, AGA AS, Porsgrunn, Norway

N-PAH and O-PAH standards (see Table B.1), CHIRON AS, Trondheim, Norway

B.3 Materials

UNIS

TE-1000-BL PUF Poly-Urethane Foam High Volume Air Sampler, Tisch Environmental, Inc., Cleves, OH, USA

Micro-quartz fiber filters, 103 mm, Munktell, Ahlstrom Germany GmbH, Nümbrecht, Germany

Quartz Microfiber filters, 101.6 mm, Whatman, GE Healthcare Life Sciences, Maidstone, United Kingdom

Polyurethane foam, D=2.5 inch, L=2 inch, Sunde Søm & Skumplast A/S, Gan, Norge

Round bottom flasks, 500 mL

Beakers and Erlenmeyer flasks of various volumes

TurboVap tubes, 200 mL with 0.5 mL endpoint stem, Biotage, Uppsala, Sweden

BLAUBRAND micropipettes intraMARK (20, 25, 50 and 100 µL), BRAND GMBH, Sigma-Aldrich, Oslo, Norway

Glass pasteur pipettes, 230mm, VWR International, Oslo, Norway

Pyrex glass tubes with screw caps (PTFE septum), 15 mL, Sigma-Aldrich, Oslo, Norway

Amber sample vials, 2.0 mL, Supelco, Sigma-Aldrich, Oslo, Norway

Screw caps, solid top with PTFE liner, Supelco, Sigma-Aldrich, Oslo, Norway

Soxhlet extraction tubes, 100 mL, with heating mantles and cooling system

TurboVap 500, Caliper Life Sciences, Waltham, MA, USA

12 Position N-EVAP Nitrogen Evaporator, Organomation, Berlin, MA, USA

Stainless steel needles, Organomation, Berlin, MA, USA

Multi-Position Analog Vortex Mixer, VWR International, Oslo, Norway

Universal 16R Centrifuge, Nerliens Meszansky AS, Oslo, Norway

CHROMABOND 10 position SPE vacuum manifold, Macherey-Nagel, Düren, Germany

CHROMABOND SPE SiOH glass cartridges, 3 mL, 500 mg, Macherey-Nagel, Teknolab, Ski, Norway

Analytical Balance XP204, Mettler Toledo, Columbus, OH, USA

Ultrasonic cleaner USC600T, VWR International, Leuven, Belgium

Laboratory Dishwasher, Ken Hygiene Systems, Broby, Denmark

High-temperature furnace HTC, Nabertherm GmbH, Lilienthal, Germany

NMBU

Analytical Balance ED224S Extend, Sartorius AG, Göttingen, Germany

MS 3 digital shaker, IKA, Staufen im Breisgau, Germany

Stainless steel needles, Organomation, Berlin, MA, USA

BLAUBRAND micropipettes intraMARK (20, 25, 50 and 100 µL), BRAND GMBH, Sigma-Aldrich, Oslo, Norway

Glass pasteur pipettes, 230mm, VWR International, Oslo, Norway

Beakers and erlenmeyer flasks of various volumes

Sample vials with fused insert (Chromacol 02-FISVG), 200 µL, Thermo Fisher Scientific, Teknolab, Ski, Norway

Screw caps, blue silicone/PTFE septum (Chromacol 9-SCK(B)-ST101), Thermo Fisher Scien-

tific, Teknolab, Ski, Norway

GC-MS: (all from Agilent Technologies, Santa Clara, CA, USA)

Gas chromatograph: 7890B GC-system

Mass spectrometer: 7000C Triple Quadrupole

Autosampler: G4513A Injector with 16-sample standalone turret

Column: Agilent J&W HP-5ms 30m x 0.25 mm, 0.25 µm film ((5%-phenyl)-methylpolysiloxane)

Injection syringe: Agilent Gold Standard Syringe, 10 µL

Liner: Agilent 5190-2293 Ultra Inert Liner with glass wool

Computer software:

Agilent MassHunter Qualitative Analysis B.07.00

Agilent MassHunter Quantitative Analysis B.07.01

Microsoft Excel 2013

MATLAB R2016b

ChemBioDraw Ultra 14.0

C Calibration curves

Calibration curves were created by least square linear regression analysis by Microsoft Excel 2013, as stated in Section 3.7.

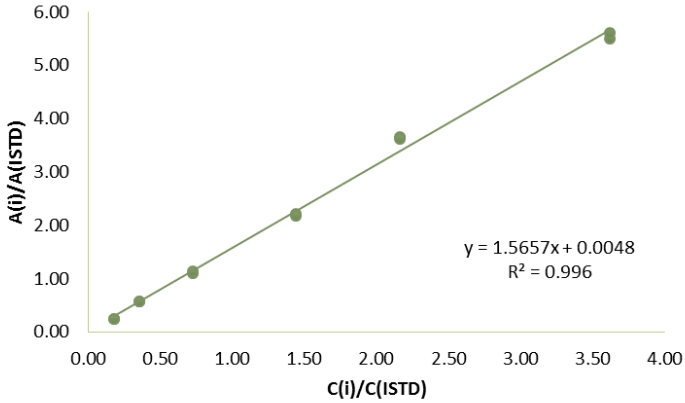

Figure C.1: 1,4-Naphthoquinone.

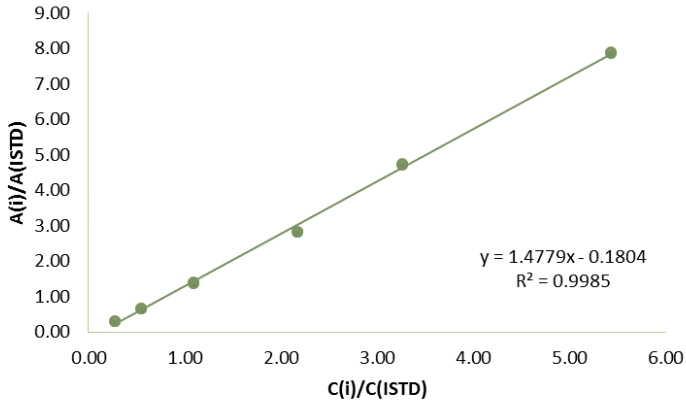

Figure C.2: 1-Nitronaphthalene.

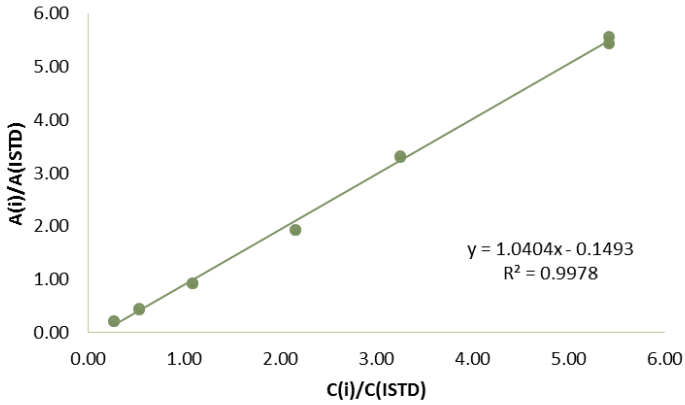

Figure C.3: 2-Nitronaphthalene.

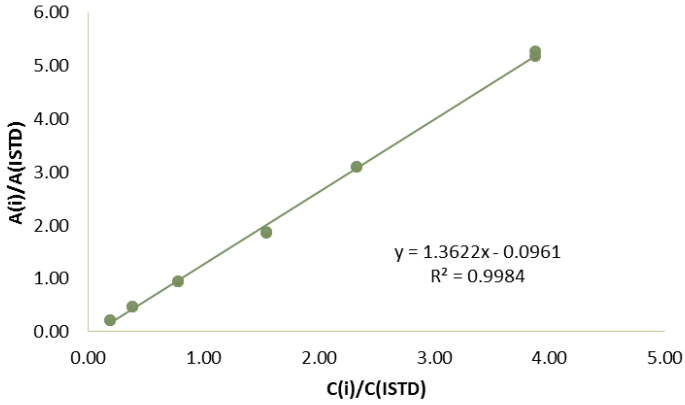

Figure C.4: 9-Fluorenone.

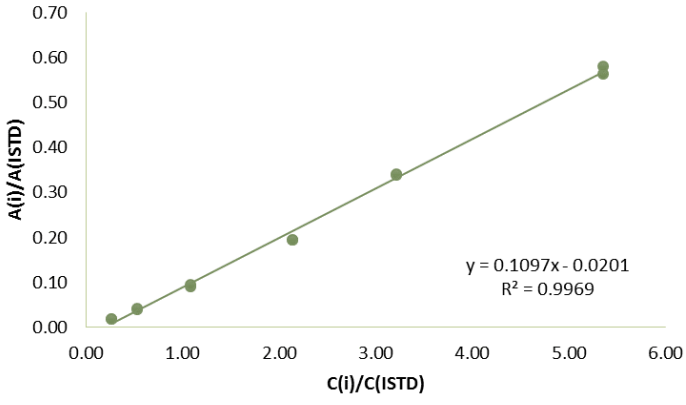

Figure C.5: 4-Nitrobiphenyl.

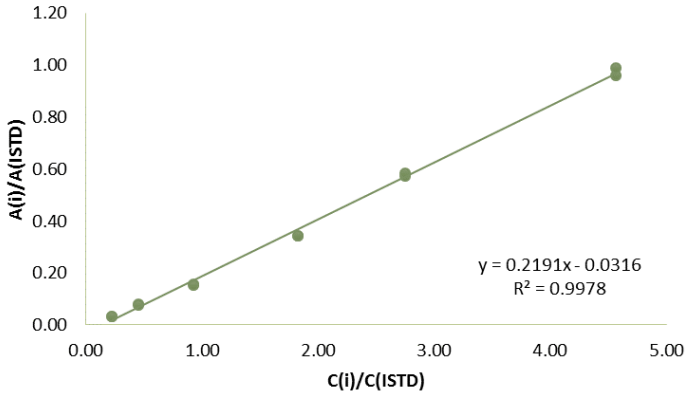

Figure C.6: 9,10-Anthraquinone.

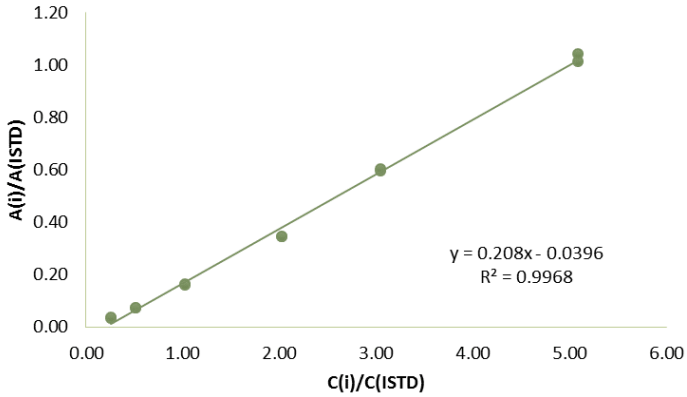

Figure C.7: 5-Nitroacenaphthene.

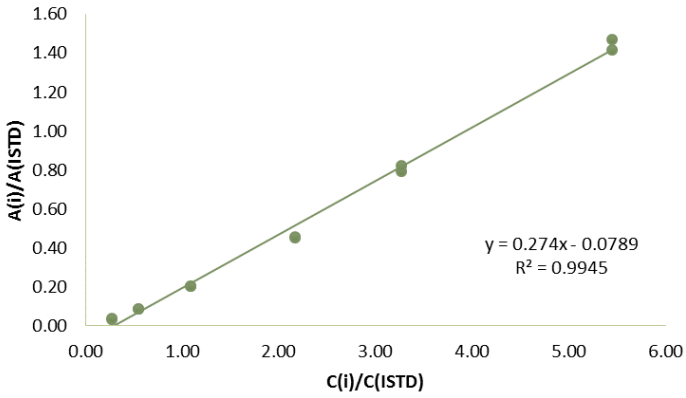

Figure C.8: 2-Nitrofluorene.

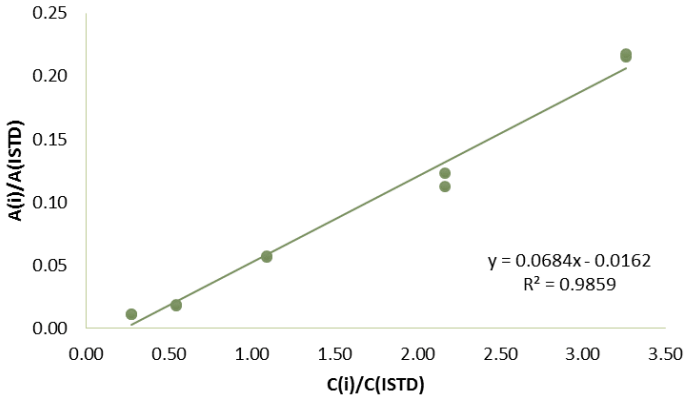

Figure C.9: 9-Nitroanthracene.

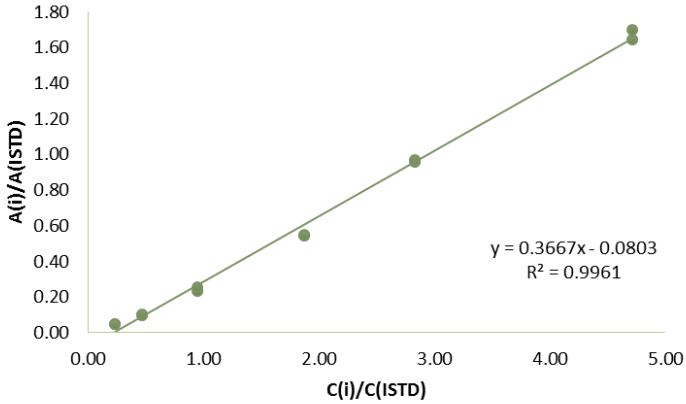

Figure C.10: 9-Nitrophenanthrene.

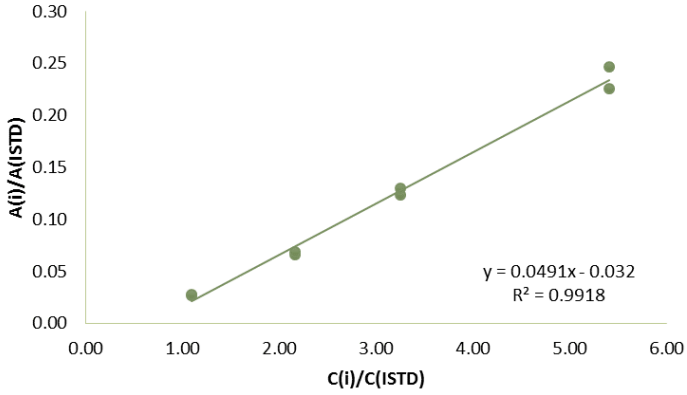

Figure C.11: 2-Nitroanthracene.

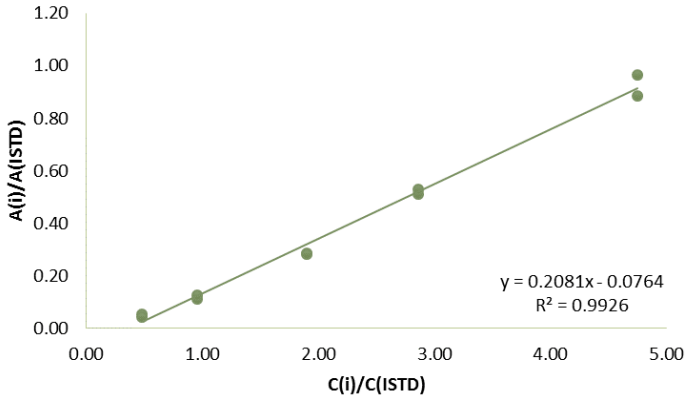

Figure C.12: Benzo[*a*]fluoren-11-one.

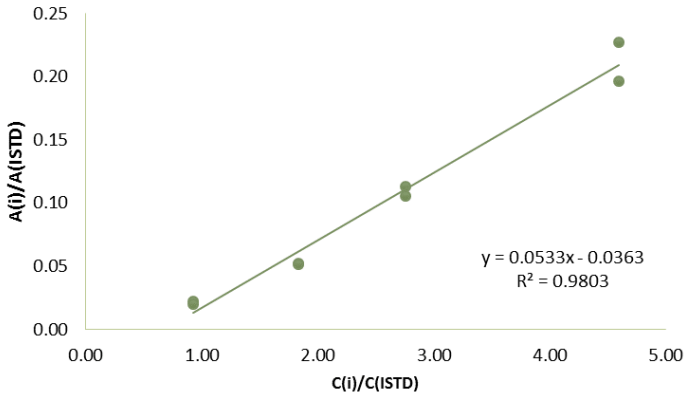

Figure C.13: Benzanthrone.

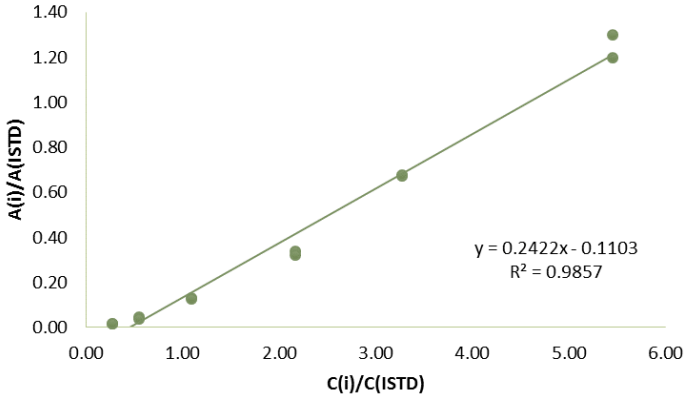

Figure C.14: 4-Nitropyrene.

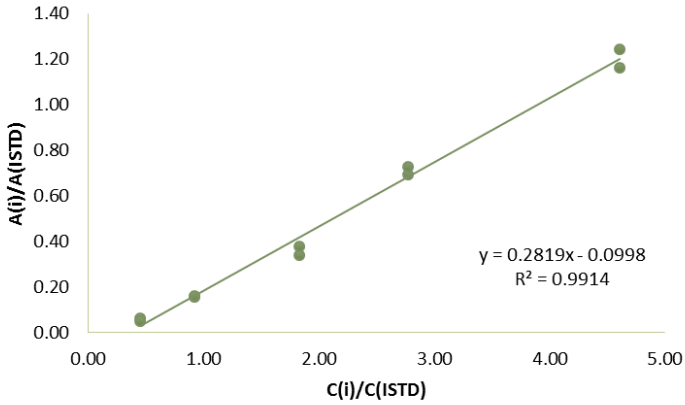

Figure C.15: 1,2-Benz[*a*]anthraquinone.

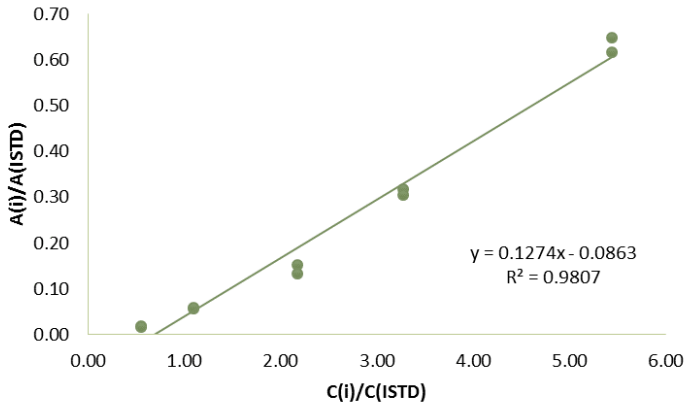

Figure C.16: 1-Nitropyrene.

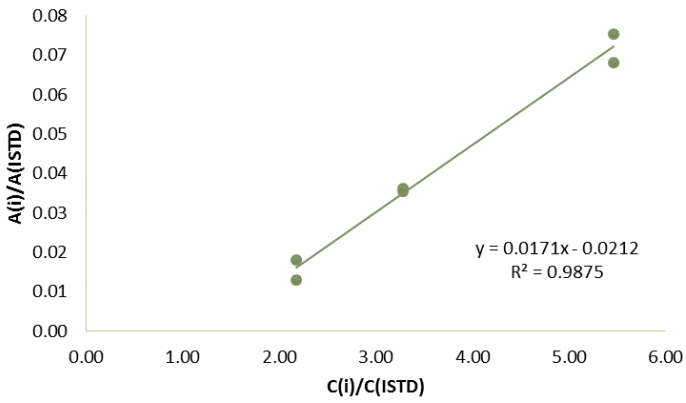

Figure C.17: 2-Nitropyrene.

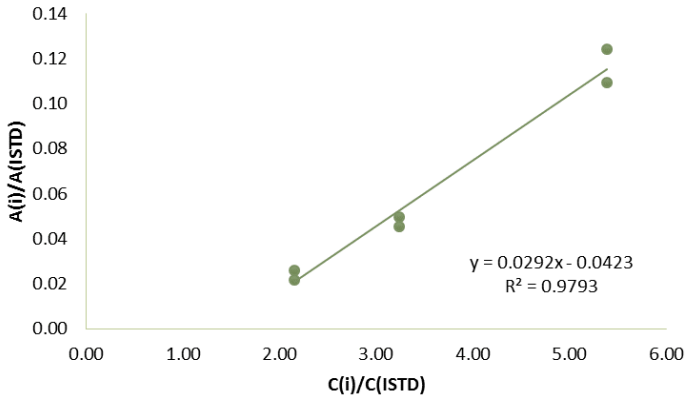

Figure C.18: 7-Nitrobenz[*a*]anthracene.

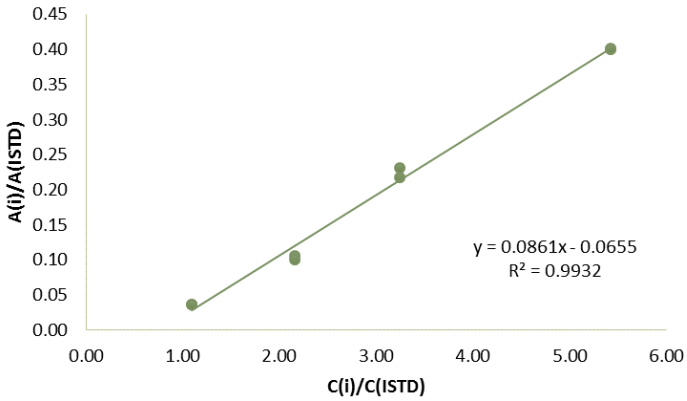

Figure C.19: 6-Nitrochrysene.